An Engineered *orco* Mutation Produces Aberrant Social Behavior and Defective Neural Development in Ants
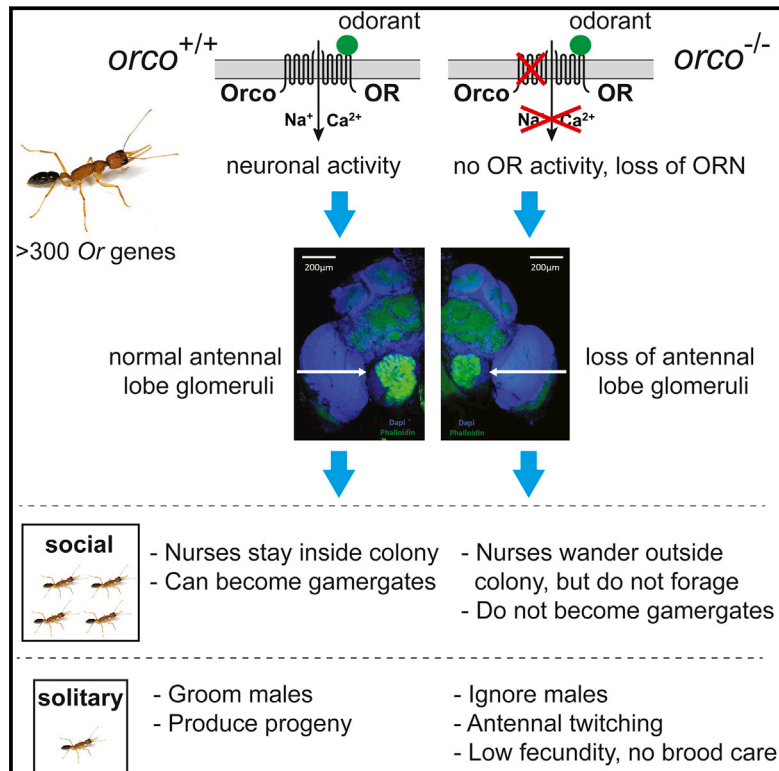
Graphical Abstract

Highlights

- Genetics was established in the ant *Harpegnathos saltator*

- A mutation in *orco* reduces ant responses to general odorants

- *orco* mutant ants display asocial behavior as well as defective reproduction

- *orco* mutants display disrupted development of ORNs and of their projections

Authors

Hua Yan, Comzit Opachaloemphan, Giacomo Mancini, ..., Jürgen Liebig, Danny Reinberg, Claude Desplan

Correspondence

bergers@mail.med.upenn.edu (S.L.B.), juergen.liebig@asu.edu (J.L.), danny.reinberg@nyumc.org (D.R.), cd38@nyu.edu (C.D.)

In Brief

Development of the first line of mutant ants using CRISPR/Cas technology reveals what happens inside a colony when ants lose the ability to recognize odors.

An Engineered *orco* Mutation Produces Aberrant Social Behavior and Defective Neural Development in Ants

Hua Yan,[1,7] Comzit Opachaloemphan,[1,8] Giacomo Mancini,[2,8] Huan Yang,[1] Matthew Gallitto,[1] Jakub Mlejnek,[2] Alexandra Leibholz,[2] Kevin Haight,[3] Majid Ghaninia,[3] Lucy Huo,[2] Michael Perry,[2] Jesse Slone,[4] Xiaofan Zhou,[4] Maria Traficante,[2] Clint A. Penick,[3] Kelly Dolezal,[3] Kaustubh Gokhale,[3] Kelsey Stevens,[2] Ingrid Fetter-Pruneda,[5] Roberto Bonasio,[6] Laurence J. Zwiebel,[4] Shelley L. Berger,[6,*] Jürgen Liebig,[3,*] Danny Reinberg,[1,7,*] and Claude Desplan[2,9,*]

[1]Department of Biochemistry and Molecular Pharmacology, New York University School of Medicine, New York, NY 10016, USA
[2]Department of Biology, New York University, New York, NY 10003, USA
[3]School of Life Sciences, Arizona State University, Tempe, AZ 85287, USA
[4]Department of Biological Sciences, Vanderbilt University, Nashville, TN 37235, USA
[5]Laboratory of Social Evolution and Behavior, The Rockefeller University, New York, NY 10065, USA
[6]Penn Epigenetics Institute, Departments of Cell and Developmental Biology, Genetics, and Biology, University of Pennsylvania Perelman School of Medicine, Philadelphia, PA 19104, USA
[7]Howard Hughes Medical Institute, New York University School of Medicine, New York, NY 10016, USA
[8]These authors contributed equally
[9]Lead contact
*Correspondence: bergers@mail.med.upenn.edu (S.L.B.), juergen.liebig@asu.edu (J.L.), danny.reinberg@nyumc.org (D.R.), cd38@nyu.edu (C.D.)
http://dx.doi.org/10.1016/j.cell.2017.06.051

SUMMARY

Ants exhibit cooperative behaviors and advanced forms of sociality that depend on pheromone-mediated communication. Odorant receptor neurons (ORNs) express specific odorant receptors (ORs) encoded by a dramatically expanded gene family in ants. In most eusocial insects, only the queen can transmit genetic information, restricting genetic studies. In contrast, workers in *Harpegnathos saltator* ants can be converted into gamergates (pseudoqueens) that can found entire colonies. This feature facilitated CRISPR-Cas9 generation of germline mutations in *orco*, the gene that encodes the obligate co-receptor of all ORs. *orco* mutations should significantly impact olfaction. We demonstrate striking functions of Orco in odorant perception, reproductive physiology, and social behavior plasticity. Surprisingly, unlike in other insects, loss of OR functionality also dramatically impairs development of the antennal lobe to which ORNs project. Therefore, the development of genetics in *Harpegnathos* establishes this ant species as a model organism to study the complexity of eusociality.

INTRODUCTION

Among the most fascinating and enigmatic phenomena in biology is the process by which environmental stimuli drive animal behavior through sensory neuron perception. Eusocial animals, including ants, live in highly sophisticated societies and display a rich repertoire of social behaviors because of the striking division of labor among distinct castes. Most ant castes are established during development in diploid females, while normally, the only role for haploid males is reproduction (Hölldobler and Wilson, 1990). However, the ponerine ant species *Harpegnathos saltator* displays strong adult phenotypic plasticity: when a queen dies or is removed from a colony, workers compete via antennal dueling, and the most frequent duelers become reproductive gamergates (pseudoqueens) (Bonasio, 2012; Hölldobler and Wilson, 2008; Peeters et al., 2000; Sasaki et al., 2016; Yan et al., 2014). While these gamergates are not morphologically different from workers, they exhibit queen-like physiology and behavior (e.g., egg-laying and a dramatically extended lifespan). This plasticity is likely induced by the deprivation of queen pheromones normally communicated via olfactory processes to repress the gamergate transition (Figure 1A). Indeed, olfaction regulates multiple behaviors in eusocial insects (Ozaki et al., 2005; Sharma et al., 2015), with communication between ant individuals being mediated in part by cuticular hydrocarbons (CHCs) and other pheromones, such as sex, alarm, or trail pheromones (Blomquist and Bagnères, 2010; Leonhardt et al., 2016; Van Oystaeyen et al., 2014). In *Harpegnathos*, CHC profiles display a clear shift to longer chain hydrocarbons when workers become reproductive gamergates (Liebig et al., 2000). Such a defined variation suggests that queen and gamergate CHCs may serve as pheromones to suppress worker ovary growth and regulate worker-specific behaviors (Sharma et al., 2015; Van Oystaeyen et al., 2014). In addition, different profiles of CHCs in nestmates versus non-nestmates in *Camponotus* ants induce aggression against non-nestmates (Ozaki et al., 2005; Sharma et al., 2015).
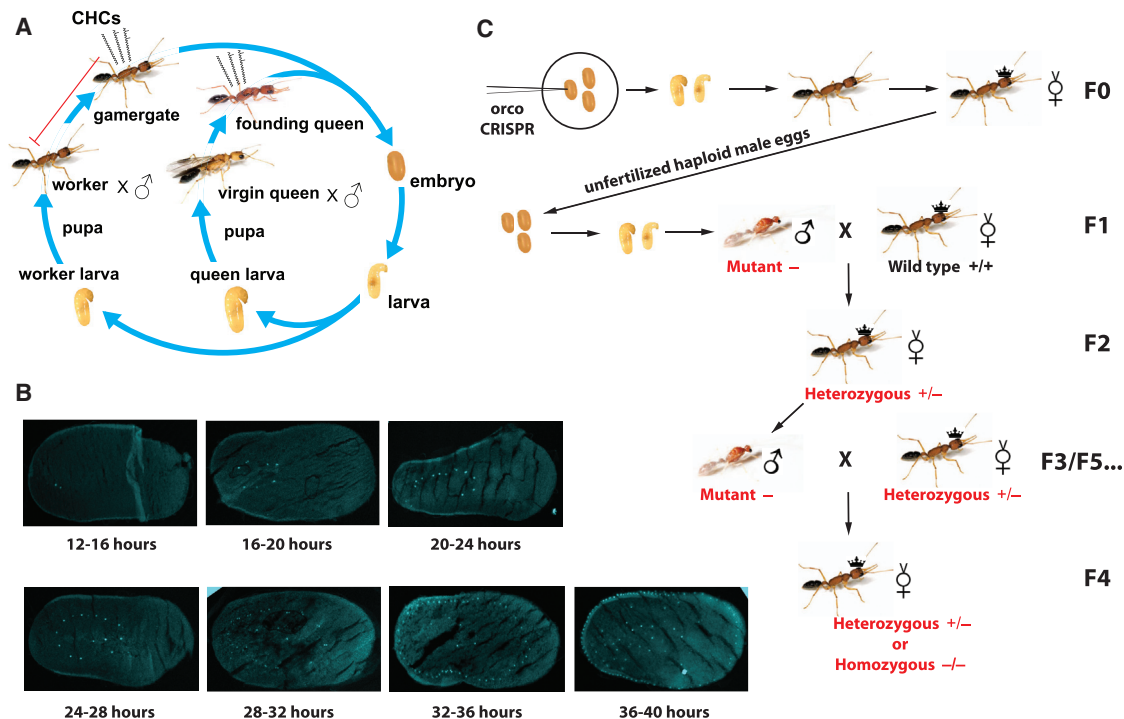
Figure 1. *Harpegnathos* Life Cycle, Early Embryo Development, and Propagation of the Mutant Allele
(A) The female embryos develop into larvae. At the fourth instar (Penick et al., 2012), the larvae differentiate into queen versus worker larvae. The former develop into callow virgin queens with wings that can found a new colony, while the latter become workers in the nest and, when isolated in group or individually, can become gamergates and lay eggs. Certain cuticular hydrocarbons (CHCs) of a queen or a gamergate act as queen pheromones that inhibit worker reproduction.
(B) Cryosections and DAPI staining of young embryos harvested at different time points after egg deposition (AED, hours below each image).
(C) The steps to propagate mutant ants to develop hemizygous males (F3/F5) and homozygous females (F4) for phenotypic analyses. Of note, the F3 mutant males mated with F2 heterozygotes to generate F4 ants, which were half homozygotes and half heterozygotes (Table S1). The F4 heterozygotes, like F2s, also produced male mutants (F5).
See also Figure S1 and Table S1.

The olfactory sensory system in insects comprises sensory neurons that are located in the sensilla on the antennae, maxillary palps and other sensory appendages (Laissue and Vosshall, 2008). The odorant receptor neurons (ORNs) express odorant receptors (tuning odorant receptors [ORs]) that confer specificity to odorant ligands. The repertoire of tuning ORs is encoded by 60 genes in the *Drosophila melanogaster* genome (47 of which are expressed in adults) (Laissue and Vosshall, 2008). However, the family of *Or* genes is dramatically amplified in ants with over 300 *Or* genes having been identified in several ant genomes (Zhou et al., 2012). The most dramatically expanded *Or* family is the female-specific nine-exon subfamily that has been associated with the evolution of eusocial interactions (Zhou et al., 2012, 2015). Other insect chemosensory receptor gene families encoding gustatory receptors (GRs) and ionotropic glutamate receptors (IRs) have not undergone a similar expansion and remain in small numbers (Zhou et al., 2012, 2015). ORN axons project to the antennal lobe (AL) that consists of numerous globule-shaped neuropils known as glomeruli, where initial synaptic integration occurs before olfactory information is sent via projection neurons to the mushroom body and the lateral horn in the central brain (Wicher, 2015). The *Drosophila* AL contains only 42 main glomeruli (Laissue and Vosshall, 2008), while over 400 glomeruli were

identified in *Camponotus floridanus* (Zube and Rössler, 2008) and in *Ooceraea biroi* (McKenzie et al., 2016), with more in females than in males (Hoyer et al., 2005; McKenzie et al., 2016). Indeed, in *Ooceraea*, the female-specific nine-exon ORNs project to a large cluster of glomeruli (T6), which are overrepresented in female ALs compared to males in both *Ooceraea* and *Camponotus* (McKenzie et al., 2016; Zube and Rössler, 2008).

Orco is the highly conserved olfactory co-receptor that forms an obligate heterodimer with all insect tuning ORs (Nakagawa et al., 2012; Vosshall and Hansson, 2011; Zhou et al., 2012). The OR-Orco dimers function as ligand-gated ion channels that activate the ORNs upon odorant binding (Benton et al., 2006). Therefore, loss of function in the *orco* gene leads to the loss of all OR-mediated chemosensation. In *Drosophila* and other insects (DeGennaro et al., 2013; Koutroumpa et al., 2016; Larsson et al., 2004; Li et al., 2016; Yang et al., 2016), *orco* is a non-essential gene whose disruption leads to dramatic reductions in olfactory sensitivity. Mutations in *orco* abolish the behavioral and electrophysiological responses to a number of general odorants in *Drosophila* (Larsson et al., 2004).

In mammals, a very large family of *Or* genes (>1,000) encode G-protein-coupled receptors (GPCRs) with no evolutionary relationship to insect ORs. However, like in insects, ORNs typically

express only one OR and all ORNs expressing a given OR project to the same glomeruli in the olfactory bulb. Given the very large number of ORs in mammals, their activity is believed to be required for the ORNs to find their correct glomeruli in the olfactory bulb (Mombaerts, 2006; Yu et al., 2004). In *Drosophila*, with only 42 main glomeruli (Laissue and Vosshall, 2008), the presence of an OR is not required for ORNs to project to their correct glomerulus. Indeed, *Drosophila orco* mutants do not exhibit altered glomerulus number or morphology (Chiang et al., 2009; Larsson et al., 2004). This suggests that, unlike in mammals, the *Drosophila* brain is largely hardwired by genetic programs and the anatomical features of the *Drosophila* olfactory glomeruli develop normally in an ORN activity-independent manner. It is not known whether this hardwiring feature is specific for *Drosophila* or can be generalized to other solitary or eusocial insects.

Functional studies in ants would be significantly enhanced by the ability to genetically manipulate pathways by mutagenesis and transgenesis. Unlike most eusocial insects wherein only the queen in the colony can transmit the genetic information to the next generation, any worker in *Harpegnathos* can be mated and converted to a reproductive gamergate, thereby starting a whole new colony (Liebig et al., 1998). This unique feature of this eusocial insect, along with the availability of its genome sequence (Bonasio et al., 2010), provides a strong platform for attempting to generate, propagate, and analyze mutants. Despite numerous studies that highlight the important role of olfaction in insect societies (reviewed in Leonhardt et al. [2016]), genetic tests to examine the impact of olfactory impairment on eusocial colony organization are still lacking. Therefore, we developed genetics in *Harpegnathos* by targeting the *orco* gene for mutagenesis. Strikingly, the mutant ants displayed a variety of behavioral and neuroanatomical phenotypes as described below.

RESULTS

Generation of *orco* Knockout Ants Using CRISPR

To maximize the chances for successful genome editing with CRISPR, we sought the best stage (developmental time) at which to inject *Harpegnathos* embryos so that small guide RNAs (sgRNAs) and Cas9 protein would have access to as many nuclei as possible in the future germline cells. The development of eusocial insects is longer compared to solitary insects such as *Drosophila* (Yan et al., 2014). In *Harpegnathos saltator*, the time between oviposition to imago eclosion takes 75 days at 25°C, with embryonic development taking 29 days (Figure 1A). The ideal time for genome editing by microinjection is the syncytial stage, when nuclei divide without cytokinesis (Henderson, 2004). However, the timing of this phase in *Harpegnathos* was unknown. We visualized embryos during early embryonic development and found that they reached gastrulation ~48 hr after egg deposition (AED) (Figure S1A). Nuclear staining of early embryo sections revealed that the syncytial phase lasted from 12 to 36 hr AED (Figure 1B). Based on these observations, we chose this time range to deliver sgRNAs and Cas9 by lateral microinjections (Watanabe et al., 2014). After injection, the embryos were maintained on agar plates until the first hatching. Freshly hatched larvae were transferred to a small wild-type (WT)

colony to be reared into pupae and adults by nursing workers (Figures S1B and S1C).

Orco is a seven-transmembrane domain protein, with its N terminus located at the intracellular space (Figure 2A). We used Cas9 protein (PNA Bio) and single or multiple *in vitro* synthesized sgRNAs to target the first exon of the *Harpegnathos orco* gene, 50 nucleotides downstream of the translational initiation codon (ATG; Figure 2B). The target was validated after extracting genomic DNA from injected embryos followed by PCR and pGEM cloning, which identified multiple short deletions from a single sgRNA (Figure 2B). Longer deletions between the two target sites were found when two sgRNAs were co-injected (Figure S2A). The efficiency of somatic mutagenesis reached approximately 40%, as evidenced by MiSeq deep sequencing (Kistler et al., 2015) of genomic DNA derived from whole embryos sacrificed 3 days after injections (Figure S2B).

Among social insects, *Harpegnathos saltator* is uniquely suitable for the establishment and maintenance of mutant lines given its unusual caste plasticity (Yan et al., 2014). Specifically, any female adult individual, most notably any adult mutant, can be converted to a reproductive gamergate and can therefore transmit the modified allele to its progeny. The gamergate phenotype can be induced in a social context by removing the queen (or the previously established gamergates) from a colony, or by completely isolating individual workers that, sensing the absence of the queen, become so-called "solitary gamergates." Worker ovaries are atrophic and only have the germarium (Figure S1D), but become fully activated within 20 days after isolation, when the solitary gamergate begins to lay eggs (Liebig et al., 1998; Peeters et al., 2000). Isolated workers are unmated and their unfertilized eggs develop into haploid males.

We converted isolated workers derived from injected embryos into gamergates (F0) and their haploid male progeny (F1) were genotyped by clipping their forewings and sequencing the CRISPR target site (Figures 1C and 2C). One of the *orco* mutations comprised a deletion of two nucleotides in the first exon, resulting in a frameshift at codon 17 located at the N-terminal intracellular segment (Figure 2A), and a premature stop codon (Figure 2C), thus yielding a putative null mutant. The *orco* haploid mutant males did not display visible morphological or behavioral phenotypes and were fully fertile (see below). We out- and backcrossed this animal to obtain F4 homozygous females (see below and STAR Methods, Figure 1C; Table S1) and confirmed the absence of detectable Orco peptide in these homozygous individuals using mass spectrometry (Figures 2D, S2C, and S2D) and thus, that the frameshift resulted in a complete loss of function. In addition, the genetic inheritance followed Mendelian rules, as almost equal numbers of F3 WT versus mutant males, and F4 heterozygous versus homozygous females were observed (Table S1). Workers do not have wings and could be genotyped only after being sacrificed. Thus, all subsequent experiments were performed blind.

Orco Is Required for Chemical Responses

In several insect species, *orco* mutants display a reduced response to general odorants (DeGennaro et al., 2013; Koutroumpa et al., 2016; Larsson et al., 2004; Li et al., 2016). To test the function of Orco in the response of workers to odorants,
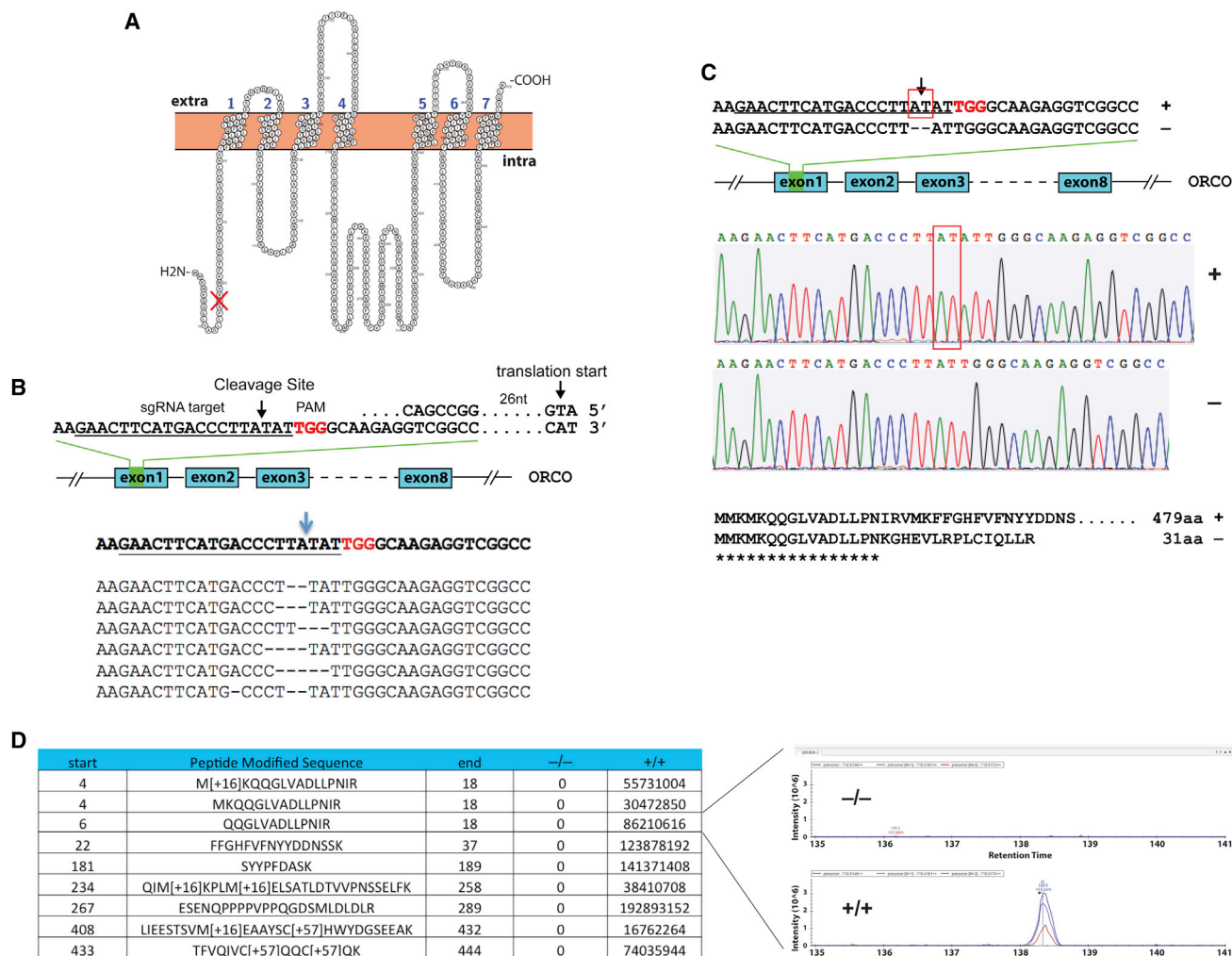
Figure 2. Development of Somatic and Germline Mutations

(A) The structure of Orco protein with seven transmembrane domains, labeled 1 to 7. The mutation is at the N terminus of the protein and is indicated by the red mark. Extra and intra, extra- and intra-cellular domains.

(B) Microinjections of *orco* CRISPR into embryos generated multiple types of short deletions. The target site in the first exon of the *orco* gene, indicated by an arrow, is located three nucleotides upstream of the PAM (TGG) sequence. The small guide RNA (sgRNA1) target sequence is underlined.

(C) The germline mutation used for this study was a 2-nucleotide AT deletion, as indicated in the sequencing chromatogram (+, WT; −, mutation). The mutation caused a frameshift at codon 17 and a premature stop codon, giving rise to the truncated protein of 31 amino acids.

(D) Mass spectrometry indicates the abundance (peak area in inset) of detected peptides from Orco protein in the WT female ant (+/+) compared to the F4 *orco* homozygous mutant ant (−/−). Each row represents a fragment of the WT Orco protein sequence with its start and end amino acid positions.

See also Figure S2.

we established a bioassay that scores for antennal retraction after odorant delivery (Figure S3A). In ants and other insects, seven odorants are known as alarm, or attractant/repellent pheromones (Böröczky et al., 2013; Capinera, 2004; de Bruyne et al., 2001; Ditzen et al., 2008; Duffield et al., 1977; Zhao et al., 2010). These chemicals induce significant antennal retraction responses in WT *Harpegnathos* (Figure S3B). Fourteen F4 putative *orco* mutant ants were paired (see STAR Methods) with 14 WT control ants and their responses to different odorants were analyzed in parallel. While the WT ants robustly responded to these odorants, the F4 ants displayed bimodal responses, which allowed us to predict their genotypes. Statistical analyses for

each odorant showed that the *orco* homozygous mutants displayed significantly lower responses to all odorants compared to heterozygous ants (Figures 3A and 3B; Movie S1). Thus, genome editing of the *orco* locus resulted in a loss-of-function mutation that was transmitted through the germline in an ant.

orco Mutant Ants Display Behavioral Phenotypes Consistent with the Loss of Pheromone Sensing

Age-based division of labor is a common phenomenon in eusocial insects. Young workers stay in the nest and nurse the brood, while older workers leave the nest and forage to bring food back to the colony (Haight, 2012; Robinson, 1987; Yan et al., 2014).
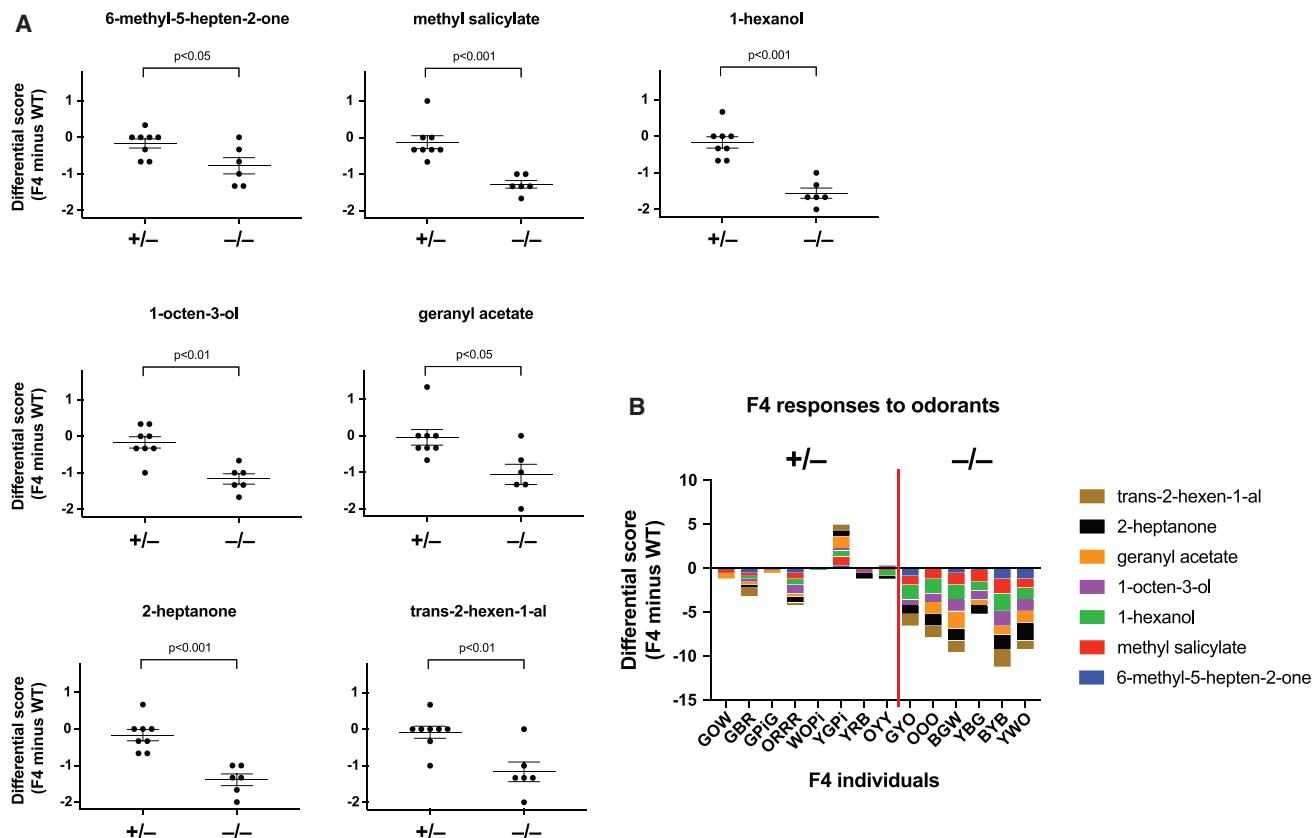
Figure 3. Reduced Antennal Responses to Odorants in *orco* Homozygous Mutant Ants

(A) The differential score (y axes) of each heterozygous (+/−, n = 8) or homozygous ant (−/−, n = 6) relative to its paired WT ant was plotted and the p value indicated. Mann-Whitney test was used for statistical analyses. Bars and error bars represent mean ± SEM.

(B) The cumulative differential scores in response to seven odorants were separated into heterozygous and homozygous groups. Each ant was named by its painted color combination (see STAR Methods). Of note, YGPi was paired with an outlier, a WT ant with low responses to odorants.

See also Figure S3 and Movie S1.

Harpegnathos ants behave similarly since newly eclosed workers remain in the nest while older workers (>100 days old) leave the nest to forage. We speculated that chemical signals within the nest might drive young workers to normally aggregate with gamergates (Movie S2) (Ali and Morgan, 1990; Depickere et al., 2004). Interestingly, young homozygous *orco* worker ants (age < 50 days) spent a much longer time outside the nest than WT and heterozygous young workers (Figure 4A; Movie S3), suggesting that the *orco* mutation caused a measurable phenotype in a distinct social behavior (leaving the colony), most likely due to a defect in sensing chemical signals in the nest. Alternatively, they might not be able to perceive the difference between the inside and the outside of the nest, which is necessary to identify the nest entrance and return inside. This is consistent with the loss of olfactory function. This wandering phenotype was not due to an early transition to forager in homozygous *orco* mutants since the ants that spent much of their time outside the nest never foraged to return crickets back to the nest (Figure 4B). In fact, these ants fed on crickets brought to the nest by WT workers. This suggests that *orco* mutants are not only impaired in their ability to detect pheromones that lead to aggregation of young workers with gamergates (Movie S2) but also in

sensing the presence of prey, such as crickets, when outside of the nest. Alternatively, the olfactory impairment might have changed their behavioral development so that they no longer act as foragers.

Loss of Orco Impairs Worker Dueling and the Transition to Gamergates

In the absence of a reproductive queen or gamergates, a large proportion of workers (30%–60%) enter a ritualized dueling behavior. While some desist rapidly, most of those that persist in dueling become gamergates and lay eggs (Sasaki et al., 2016; Gospocic et al., 2017 [this issue of *Cell*]). To address whether the *orco* mutation affected dueling and the gamergate transition, we generated a colony with 39 randomly selected young F4 putative *orco* mutant ants within a setting devoid of a queen or gamergates, and tested their ability to become gamergates. As usual, dueling started 3 days after colony setup. During the first day of dueling, 14 out of 39 workers (36%) dueled (Tables S2 and S3). This number became lower with time as some duelers returned to worker behavior (Table S3). From dueling day 3 to day 9, only six workers constantly dueled. Finally, four of them became gamergates (Figure 4C; Table S3).
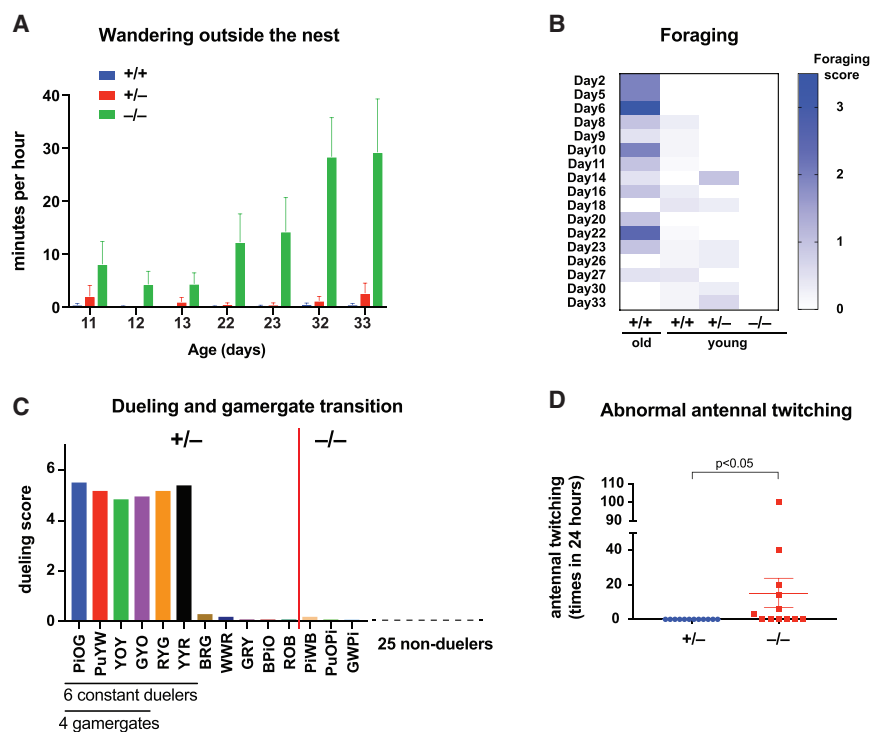
Figure 4. Behavioral Phenotypes in *orco* Homozygous Mutant Ants

(A) The time for homozygous young workers (−/−, n = 6) versus heterozygous (+/−, n = 6) and WT (+/+, n = 16) young workers to wander outside of the nest (Movie S3): p < 0.001 between homozygotes and heterozygotes; p < 0.0001 between homozygotes and WTs; p = 0.9335 between heterozygotes and WTs (two-way ANOVA with Tukey's multiple comparisons test).

(B) The wandering homozygous ants did not forage. The foraging scores are indicated in the heatmap for old WT, young WT, heterozygous, and homozygous workers (day: test day, also age of young workers). p < 0.001 between young homozygous and old WT workers (Friedman test with Dunn's multiple comparisons test).

(C) The average dueling times in 11 heterozygous duelers (left) versus 3 homozygous duelers (right) in the first 9 dueling days. The 6 constant duelers and 4 gamergates are indicated under the individual ants. See also Tables S2 and S3.

(D) Abnormal antennal twitching behavior (Movie S4) was found in 6 out of 12 individually isolated homozygotes, but not in any of the 12 heterozygotes, under the same conditions: p < 0.05 (Mann-Whitney test). Data are represented as mean ± SEM.

See also Tables S2 and S3 and Movies S2–S4.

Subsequent genotype analyses indicated that only 3 out of the 17 homozygous *orco* mutants (18%) entered dueling (Table S2), but then quickly ceased on day 2 and never became gamergates (Figure 4C; Table S3). In contrast, 11 out of the 22 heterozygotes (50%) joined dueling (Table S2). The 6 remaining duelers and the 4 final gamergates were all heterozygous (Table S3). Therefore, the homozygous and heterozygous ants display statistically significant differences not only in dueling engagement (p < 0.05, Fisher's exact test; Table S2) but also in dueling frequency (p < 0.01, Wilcoxon test; Table S3). This suggests that loss of Orco leads to the lack of proper olfactory input necessary for the continuation of appropriate dueling behavior to achieve reproductive status (Liebig et al., 2000).

In a solitary environment, the homozygous *orco* mutants also displayed another abnormal behavior: they quickly moved their antennae (Movie S4), similar to the quick antennal movement observed during dueling among workers in the transition to gamergates. This abnormal antennal twitching behavior was never observed in isolated heterozygotes (Figure 4D). This aberrant behavior is paradoxical given that the homozygous mutants rarely engaged in dueling with heterozygous workers when in a society (see above), underscoring that a functional Orco protein is required to correctly sense and respond to environmental cues (see above).

Mating and Reproduction Are Impaired in Homozygous *orco* Mutants

In *Harpegnathos*, the mating ritual begins with the female grooming the male for a few hours, until copulation begins and lasts for 20–50 s (Movie S5). *Harpegnathos* males can mate multiple times, but females mate only once in the nest (monoandry). Heterozygous females, like WT, groomed and mated with males. However, we never observed any grooming and mating behavior from homozygous mutant females, consistent with the hypothesis that sex pheromones, such as CHCs in hymenopterans (Kather and Martin, 2015), which are used to attract mates, are not sensed by *orco* mutant females.

When individually isolated, the *orco* homozygous ants, like heterozygous, were capable of laying haploid eggs, but they displayed strongly reduced fecundity. They started to lay eggs significantly later than heterozygotes (45.6 days in homozygotes versus 29.4 days in heterozygotes) (Figure 5A; Table S4) and laid 7 times fewer eggs during the first 50 days after emergence (Figure 5B; Table S4). Moreover, the homozygotes did not properly care for their brood. Although one *orco* homozygote produced larvae (Figure 5C), these larvae failed to survive and develop to pupae (Table S4). In contrast, all isolated heterozygous gamergates produced larvae (Figure 5C), pupae and adults (Table S4). Interestingly, *orco* mutant males, like WT males, were capable of mating with females to have healthy progeny (Movie S5), which allowed us to propagate the mutants (Table S1). This suggests that, unlike in females, Orco is not required in males for mating and proper reproduction inside the nest, indicating a reduced importance for OR-mediated chemosensation in contributing to the more defined male behaviors. Males are likely to require OR function at the time of mating with virgin queens from other colonies during the nuptial flight.

Homozygous *orco* mutant females were viable and healthy, but we could not evaluate their lifespan because of the long natural lifespan of *Harpegnathos* females (median
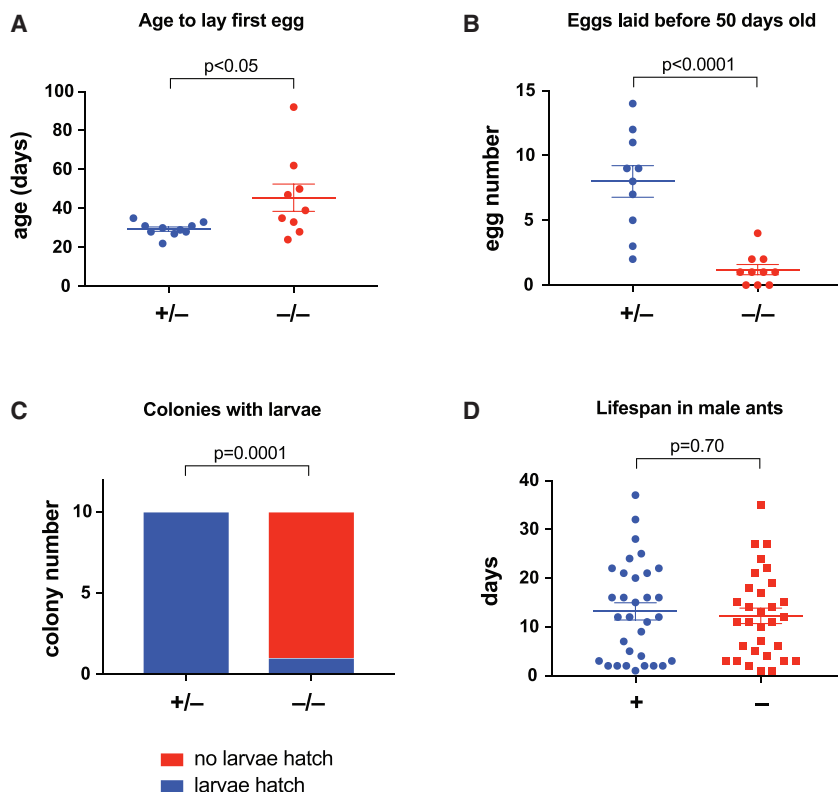
Figure 5. Defective Reproduction and Nursing in *orco* Homozygous Mutant Females but No Change in Lifespan of *orco* Mutant Males

(A) When individually isolated, the heterozygous ants (+/−, n = 10) laid the first egg at day 29.4 ± 1.1, while the homozygous mutant ants (−/−, n = 9) did so at day 45.6 ± 7.1: p < 0.05 (unpaired t test).

(B) The heterozygous ants (n = 10) laid 8.0 ± 1.2 eggs before being 50 day old, while the homozygous ants (n = 10) laid 1.2 ± 0.4 eggs before 50 days old: p < 0.0001 (unpaired t test).

(C) While all heterozygous ants (n = 10) produced larvae, only one homozygous ants (n = 10) did so: p = 0.0001 (Fisher's exact test). See also Table S4.

(D) The WT (+, n = 32) and hemizygous mutant F3 male ants (−, n = 31), which lived with individually isolated female ants, had average lifespans of 13.19 ± 1.76 days and 12.26 ± 1.58 days, respectively: p > 0.05 (unpaired t test). Data are represented as mean ± SEM.

See also Tables S1 and S4 and Movie S5.

lifespan: ∼7 months) (Haight, 2012) and since most F4 individuals were heavily manipulated for behavioral experiments. However, we did measure the lifespan of mutant and WT males. Males have a much shorter lifespan than do females. Notably, mutant males displayed similar lifespan to that of WT males (Figure 5D), suggesting that impaired OR function does not reduce survival of male ants, and that no significant off-target mutations affect their viability.

Mutation in *orco* Leads to Dramatic Decreases in the Number of ORNs and Antennal Lobe Glomeruli

In *Drosophila* and in mammals, all ORNs expressing the same *Or* gene project to the same specific glomeruli in the antennal lobes or olfactory bulb, respectively (Mombaerts, 2006; Vosshall et al., 2000). With some exceptions, each *Drosophila* ORN is believed to express only one *Or* gene (along with *orco*) and to project to one of 42 distinct glomeruli. Mutations in *orco* or manipulation of ORN activity do not alter the morphology of ORNs and the AL where ORNs project in the flies, at least within 2 days post-eclosion (Chiang et al., 2009; Larsson et al., 2004). This led to the assumption that, unlike in mammals, ORN function is not required to establish the number and shape of glomeruli that appear to be developmentally hardwired. We were therefore surprised that, while performing our studies, a similar *orco* mutant in another species of ants, *Ooceraea biroi*, a parthenogenetic ant with a peculiar phase-alternating foraging and egg laying behavior, was described as exhibiting a dramatic decrease in the number of glomeruli (reported in this issue of Cell) (Trible et al., 2017). We thus dissected the brain of old F4 ants and performed staining using Phalloidin to mark the glomeruli (Hoyer et al., 2005). The volume of the AL of *orco* homozygous *Harpegnathos* mutants was much smaller (1.30 ± 0.09 × 10^6 μm^3) than that of heterozygous (2.15 ± 0.08 × 10^6 μm^3) or WT ants (2.13 ± 0.12 × 10^6 μm^3) (Figures 6A, 6B, and S4A; Movie S6). Moreover, as was observed in *Ooceraea orco* mutant ants (Trible et al., 2017), *Harpegnathos orco* mutants had a dramatically reduced number of glomeruli: 275 (±4) glomeruli were present in WT and 270 (±11) in heterozygous, while only 62 (±2) were observed in homozygous *orco* mutants (Figure 6C). Strikingly, in homozygous *orco Harpegnathos* mutants, the diameter of the remaining individual glomeruli was 1.6 times that of heterozygous (Figure 6D). To address whether the dramatic morphological changes in glomeruli and antennal lobes in *orco* mutant ants occurred in adults due to a requirement for OR function in neural maintenance, like in *Drosophila* (Chiang et al., 2009), or during neural development, we analyzed newly eclosed F4 mutant ants (<1 day old, the youngest <2 hr old). Surprisingly, they displayed the same phenotypes like in old F4 mutants (Figure S5). These findings strongly suggest that ants, in contrast to *Drosophila*, display strong olfaction-mediated neuroanatomical plasticity during neural development. The increased size of the glomeruli in the mutant suggests that the remaining glomeruli failed to separate in the absence of Orco function.

The loss of glomeruli might also be due to the loss of the ORNs that innervate them. We therefore looked at the presence of ORNs in the antenna. In the absence of *orco* expression, it is not possible to identify OR-expressing ORNs. Therefore, we compared the number of nuclei in WT versus F4 mutant antennae, a portion of which correspond to ORN nuclei (Menuz et al., 2014). Young and old WT females displayed dense, antennal nuclei clustered under sensilla (Figures 7A and 7B) (Nakanishi et al., 2009). In contrast, young and old F4 mutants had very sparse nuclear density, which, unlike
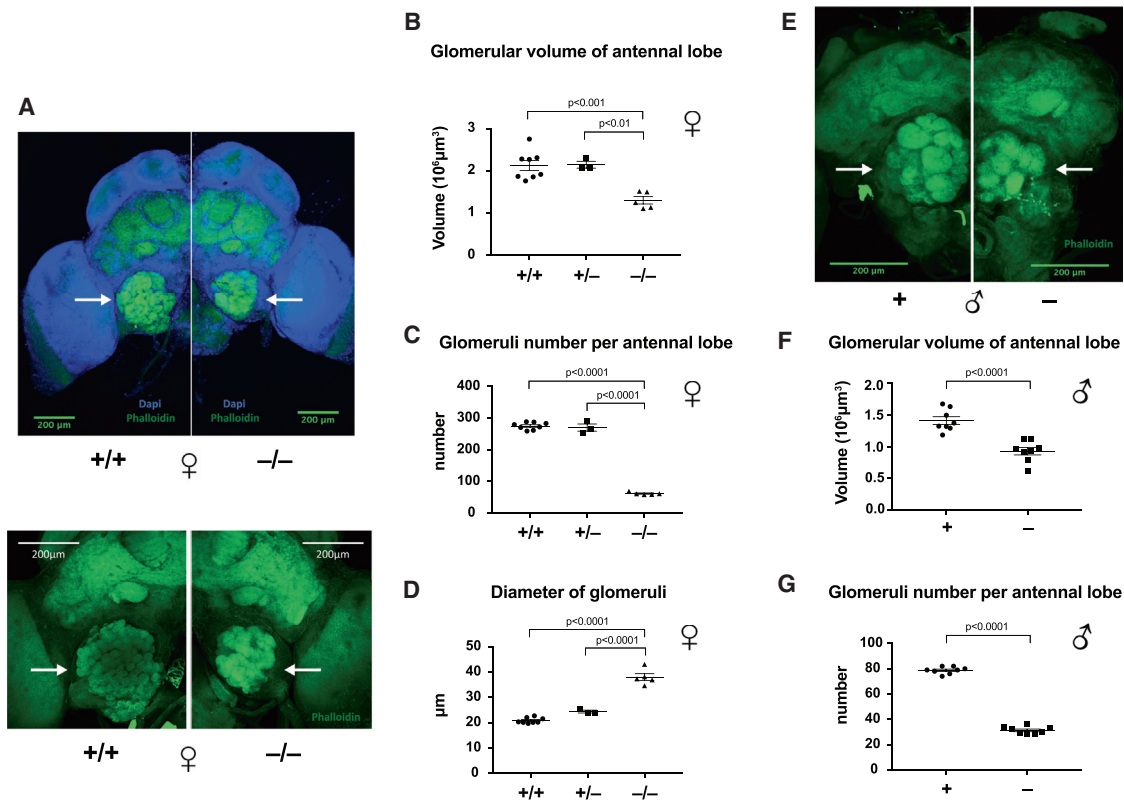
B

Glomerular volume of antennal lobe

♀

p<0.001
p<0.01

Volume ($10^6 \mu m^3$)

+/+   +/−   −/−

E

Phalloidin

200 μm   200 μm

+   ♂   −

A

Dapi
Phalloidin

200 μm   200 μm

+/+   ♀   −/−

200μm   200μm

+/+   ♀   −/−

C   **Glomeruli number per antennal lobe**

♀

p<0.0001
p<0.0001

number

+/+   +/−   −/−

D   **Diameter of glomeruli**

♀

p<0.0001
p<0.0001

μm

+/+   +/−   −/−

F   **Glomerular volume of antennal lobe**

♂

p<0.0001

Volume ($10^6 \mu m^3$)

+   −

G   **Glomeruli number per antennal lobe**

♂

p<0.0001

number

+   −

Figure 6. Neuroanatomical Phenotypes in Female and Male Mutant Ants

(A and E) The ant brain samples were stained with Phalloidin (green) and counterstained with DAPI (blue). Confocal images of two WT (+/+) versus two homozygous (−/−) old female ants (∼3 months old) are shown in (A): 10× objective (top panel) and 20X objective (bottom panel). Confocal images of WT (+) versus mutant (−) male ants using 20× objective are shown in (E). The glomerular areas of antennal lobes are indicated by arrows in (A) and (E).

(B) The average glomerular volume of left and right antennal lobes in WT (n = 8): $2.13 \pm 0.12 \times 10^6 \ \mu m^3$, heterozygous (+/−, n = 3): $2.15 \pm 0.08 \times 10^6 \ \mu m^3$, and homozygous female ants (n = 5): $1.30 \pm 0.09 \times 10^6 \ \mu m^3$.

(C) The number of glomeruli in WT: 275.2 ± 4.0, heterozygous: 270.2 ± 11.2, and homozygous female ants: 61.8 ± 1.9.

(D) The diameter of glomeruli in WT: 20.8 ± 0.4 μm, heterozygous: 24.4 ± 0.6 μm, and homozygous female ants: 38.0 ± 1.4 μm.

(F) The glomerular volume of each antennal lobe in WT (n = 8): $1.41 \pm 0.06 \times 10^6 \ \mu m^3$, and mutant male ants (n = 8): $0.93 \pm 0.06 \times 10^6 \ \mu m^3$.

(G) The number of glomeruli in WT: 78.8 ± 1.0 and mutant male ants: 31.3 ± 1.0. Female: one-way ANOVA with Tukey's multiple comparisons test; male: unpaired t test. Data are represented as mean ± SEM.

See also Figures S4 and S5 and Movies S6 and S7.

WTs, did not form recognizable clusters (Figures 7A and 7B). It is therefore likely, that OR function is required for the development and/or maintenance of ORNs. The remaining neurons in mutants innervate a small number of remaining glomeruli that might develop, like in *Drosophila*, in the absence of OR function.

Interestingly, the size of the AL of *orco* hemizygous mutant males was also significantly smaller ($0.93 \pm 0.06 \times 10^6 \ \mu m^3$) than in WT males ($1.41 \pm 0.06 \times 10^6 \ \mu m^3$) (Figures 6E, 6F, and S4B; Movie S7). The number of glomeruli was also dramatically decreased: 31 (±1) in mutants versus 79 (±1) glomeruli in WT (Hoyer et al., 2005) (Figure 6G). Male glomeruli widely varied in size with dorsal glomeruli being much larger than ventral ones (Hoyer et al., 2005). In *orco* mutant males, the dorsal and some ventral glomeruli became smaller (Figure S4C). Since *orco* mutant males exhibit normal mating inside the nest, as well as normal fertility and lifespan, the remaining glomeruli are apparently sufficient for their reproductive behavior within the nest.

We could not investigate in the lab male behavior during the nuptial flight.

DISCUSSION

Reproductive division of labor, the defining feature of eusocial animals, poses a significant challenge to generating and maintaining germline mutations in laboratory colonies because only a few individuals in a colony reproduce. The advantage of *Harpegnathos* over many other hymenopteran eusocial species is that all females can sexually reproduce after conversion to gamergate, which can be induced by social isolation (Yan et al., 2014). This characteristic provides the opportunity to effectively use gene targeting to study developmental, neuronal and behavioral plasticity in a social insect. In parallel to our studies, Daniel Kronauer and his colleagues (Trible et al., 2017) developed lines of *orco* mutants using thelytokous parthenogenesis in *Ooceraea* where all progeny are maternal clones. The
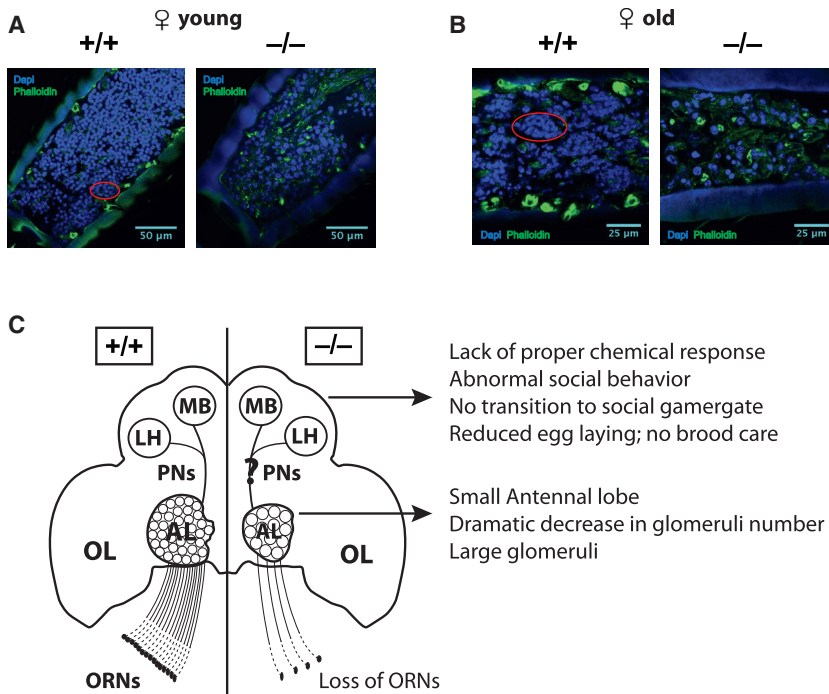
Figure 7. Loss of Odorant Receptor Neurons in Female Mutant Ants

(A) Single focal plane images of antennal flagellum (F10, the most distal flagellomere [Ghaninia et al., 2017]) in the young female ants (WT versus homozygous, <1 day old): DAPI (blue), Phalloidin (green).

(B) Images of F7 in old ants (WT versus homozygous, >3 months old). The red circles in WT panels indicate clustered nuclei.

(C) A summary of Orco function in ants: in *orco* mutant female ants, reduced number of ORNs causes a series of morphological phenotypes in the antennal lobe (AL). However, it is not clear how these changes affect the projection neurons (PNs) that innervate to the mushroom body (MB) and the lateral horn (LH). Eventually, defective olfactory sensing results in a range of abnormal behaviors and reduced capability of egg-laying and brood care. OL, optic lobe.

phenotypes they obtained with this very different species that diverged from *Harpegnathos* 120 million years ago (McKenzie et al., 2014) are fully consistent with our own observations. Thus, taken together, these two studies describe the first functional analyses using genetic mutants in eusocial insects. *Harpegnathos*, in particular, provides an apt species to utilize as a genetic model organism as the ability to perform genetic crosses will foster the development of more sophisticated genetic tools similar to those available in *Drosophila* (e.g., UAS-GAL4-inducible lines and multiple mutants). Such a repertoire would then allow for an expansion of genetic analyses to further our understanding of the genetic and epigenetic regulation of social behavior.

In ants, queen pheromones play a major role in suppressing worker reproduction (Van Oystaeyen et al., 2014). During the worker to gamergate transition in *Harpegnathos*, the CHC profile shifts to longer chain hydrocarbons, which mimics the CHC profile of the queen. Some of these long chain hydrocarbons most likely act as queen pheromones (Liebig et al., 2000), the absence of which triggers dueling in workers. The *orco* mutant workers display a series of behavioral phenotypes that are consistent with the loss of olfactory function (Figure 7C): (1) they display reduced response to general odorants; (2) they wander out of the social group and are unable to forage successfully; (3) they appear to be largely unable to communicate with conspecifics; (4) they exhibit a dysfunctional behavior in isolation, consisting of abnormal antennal twitching, i.e., quick movement of antennae that resemble dueling, despite the absence of other ants; (5) they fail to fully engage in dueling and never transition to gamergates in the presence of other ants; (6) they do not produce progeny because they lay very few eggs and do not tend to them; and (7) they ignore the presence of males and

fail to mate, presumably because they cannot detect the male sex pheromones.

In addition, and similar to the observations in *Ooceraea* (Trible et al., 2017), loss of Orco-dependent ORNs and OR signaling resulted in a dramatic decrease in the size of the antennal lobes in both males and female *Harpegnathos*, as well as in the number of glomeruli, linking neuroanatomy to Orco function in these insects (Figure 7C). Only a small proportion (31 out of 79 in *Harpegnathos* males; 62 out of 275 in females) of glomeruli remained in the absence of *orco* function. The remaining glomeruli in the *orco* mutant ants could be those innervated by GR (gustatory receptor)- or IR (ionotropic receptor)-expressing ORNs, which remain functional in the absence of *orco*-dependent OR transduction. In mosquitoes and *Drosophila*, a significant proportion of AL glomeruli are targeted by neurons expressing GRs or IRs (Benton et al., 2009; Jones et al., 2007; Riabinina et al., 2016). In fact, significant chemosensory responses still remained in the *Harpegnathos orco* homozygous workers, as these mutants, like their heterozygous and WT counterparts, showed timid behavior toward the reproductive gamergates, and did not duel or lay eggs when in a stable colony. However, the *Harpegnathos* genome only has 17 GR and 23 IR genes (Zhou et al., 2012), suggesting that not all remaining glomeruli (62) in *orco* mutants are innervated by GR- and IR- expressing ORNs. Therefore, some of the remaining ORNs in female mutants are likely to be OR-expressing ORNs. This raises the interesting possibility that ants pattern their antennal lobe through two distinct mechanisms underlying development of the olfactory system: one that is Orco dependent and another that is ancestral in insects and is independent of Orco function, like in *Drosophila*. The latter might correspond to the remaining glomeruli in our mutants. This type of patterning is possible when a limited number of ORNs can connect to their cognate glomeruli using typical guidance molecules such as N-cadherin, teneurins, plexins, neuropilins, and semaphorins (Hong et al., 2012; Hummel and Zipursky, 2004; Imai et al., 2009; Sakano, 2010; Sweeney et al., 2007). However, with the expansion of the nine-exon OR family in ants (Zhou et al.,

2012), it would not be possible to pattern several hundred types of ORNs with a Sperry-type mechanism (Sperry, 1963); functional ORNs might thus be required as a second mechanism that might promote the development or maintain the survival of ORNs before eclosion and subsequently split proto-glomeruli into multiple glomeruli, as a function of such activity. The presence of considerably fewer glomeruli in males correlates with the lack of expression of nine-exon ORs and thus might reflect less reliance on activity-dependent patterning. While the *orco* mutation certainly causes the loss of OR activity, Orco might play additional roles in ants, perhaps similar to the dual roles of Rhodopsin1 in *Drosophila*: Rh1 not only transduces the light signal, but it is also required to allow the establishment and maintenance of rhabdomeric membranes (Chang and Ready, 2000).

A similar mechanism has been proposed for the formation of the more than 1,000 pairs of glomeruli in mice that require the activity of ORs. The mechanisms that mediate the projection of ORNs to specific glomeruli remain unknown. It should be noted that the structure of ORs in insects, which are cation channels, is very different from that of mammalian ORs, which are GPCRs. Yet, the two signal transduction cascades might have undergone convergent evolution to direct the neurons to their target glomeruli. In mammals, although the gross anatomy of the adult brain does not change dramatically in the absence of electrophysiological activity, significant changes can be observed in several parts of the brain when activity is prevented during critical periods (Espinosa and Stryker, 2012; Hubel and Wiesel, 1979). Furthermore, neural stem cells (NSCs) that contribute to adult neurogenesis in two brain regions, the hippocampus and the olfactory bulb (OB), are regulated by environmental input throughout life (Suh et al., 2009). In contrast, the insect brain is widely believed to be more hardwired, and to depend less on activity patterning than the mammalian brain (Hassan and Hiesinger, 2015; Jefferis et al., 2001). For example, in the moth *Manduca sexta*, odorant-induced ORN activity appears after the development of the 64 glomeruli (Oland and Tolbert, 1996) and thus, is unlikely to play a role. Therefore, the *orco* phenotype in ants might be one of the first examples of activity-driven patterning in insects (Petsakou et al., 2015).

Future investigations into *Harpegnathos orco* mutants will address at what stage during development the activity of *orco* and ORN is required for the establishment/maintenance of ORNs themselves and of glomeruli, as well as whether and how loss of ORNs and glomeruli affects the establishment and maintenance of projection neurons (PNs) and their innervation to the mushroom body (MB) and the lateral horn (LH) (Figure 7C). To assess whether activity-dependent neuroanatomical plasticity is conserved in insects, it will be useful to analyze non-eusocial insects, like the solitary parasitoid wasp *Nasonia vitripennis*, which also possesses a much larger number of *Or* genes than *Drosophila* (Zhou et al., 2012). Of note, CRISPR-mediated mutagenesis in *Nasonia* has been achieved in our laboratory (unpublished data). Taken together, the future studies of the olfactory system in hymenopteran insects will provide insights toward understanding the function of the expanded ORs family in regulating neuronal and behavioral plasticity. Furthermore, *Harpegnathos* as an established genetic model organism in eusocial insects will facilitate the functional analysis of genes that are implicated in the regulation of eusociality.

STAR★METHODS

Detailed methods are provided in the online version of this paper and include the following:

- KEY RESOURCES TABLE
- CONTACT FOR REAGENT AND RESOURCE SHARING
- EXPERIMENTAL MODEL AND SUBJECT DETAILS
  - Regular maintenance of *Harpegnathos* ant colonies
  - Maintenance of the mutant allele and development of homozygous mutant ants
- METHOD DETAILS
  - Embryo injections and post-injection maintenance
  - Genotyping of embryo, larval and adult tissues
  - Mass spectrometry
  - Immunohistochemistry of embryo nuclei and adult brain, ovary and antennae
  - Behavioral responses to multiple chemicals
  - Analyses of ant behavior, egg laying and lifespan
  - Measurement of antennal lobes
- QUANTIFICATION AND STATISTICAL ANALYSIS

REFERENCES

Ali, M.F., and Morgan, E.D. (1990). Chemical communication in insect communities - a guide to insect pheromones with special emphasis on social insects. Biol. Rev. Camb. Philos. Soc. *65*, 227–247.

Benton, R., Sachse, S., Michnick, S.W., and Vosshall, L.B. (2006). Atypical membrane topology and heteromeric function of Drosophila odorant receptors in vivo. PLoS Biol. *4*, e20.

Benton, R., Vannice, K.S., Gomez-Diaz, C., and Vosshall, L.B. (2009). Variant ionotropic glutamate receptors as chemosensory receptors in Drosophila. Cell *136*, 149–162.

Blomquist G.J. and Bagnères A.-G., eds. (2010). Insect Hydrocarbons Biology, Biochemistry, and Chemical Ecology (Cambridge University Press).

Bolte, S., and Cordelières, F.P. (2006). A guided tour into subcellular colocalization analysis in light microscopy. J. Microsc. *224*, 213–232.

Bonasio, R. (2012). Emerging topics in epigenetics: ants, brains, and noncoding RNAs. Ann. N Y Acad. Sci. *1260*, 14–23.

Bonasio, R., Zhang, G., Ye, C., Mutti, N.S., Fang, X., Qin, N., Donahue, G., Yang, P., Li, Q., Li, C., et al. (2010). Genomic comparison of the ants *Camponotus floridanus* and *Harpegnathos saltator*. Science *329*, 1068–1071.

Böröczky, K., Wada-Katsumata, A., Batchelor, D., Zhukovskaya, M., and Schal, C. (2013). Insects groom their antennae to enhance olfactory acuity. Proc. Natl. Acad. Sci. USA *110*, 3615–3620.

Capinera, J.L. (2004). Encyclopedia of Entomology (Kluwer Academic).

Chang, H.Y., and Ready, D.F. (2000). Rescue of photoreceptor degeneration in rhodopsin-null Drosophila mutants by activated Rac1. Science *290*, 1978–1980.

Chiang, A., Priya, R., Ramaswami, M., Vijayraghavan, K., and Rodrigues, V. (2009). Neuronal activity and Wnt signaling act through Gsk3-beta to regulate axonal integrity in mature Drosophila olfactory sensory neurons. Development *136*, 1273–1282.

de Bruyne, M., Foster, K., and Carlson, J.R. (2001). Odor coding in the Drosophila antenna. Neuron *30*, 537–552.

DeGennaro, M., McBride, C.S., Seeholzer, L., Nakagawa, T., Dennis, E.J., Goldman, C., Jasinskiene, N., James, A.A., and Vosshall, L.B. (2013). orco mutant mosquitoes lose strong preference for humans and are not repelled by volatile DEET. Nature *498*, 487–491.

Depickere, S., Fresneau, D., and Deneubourg, J.L. (2004). A basis for spatial and social patterns in ant species: Dynamics and mechanisms of aggregation. J. Insect Behav. *17*, 81–97.

Ditzen, M., Pellegrino, M., and Vosshall, L.B. (2008). Insect odorant receptors are molecular targets of the insect repellent DEET. Science *319*, 1838–1842.

Duffield, R.M., Brand, J.M., and Blum, M.S. (1977). 6-methyl-5-hepten-2-one in formica species - identification and function as an alarm pheromone (Hymenoptera-Formicidae). Ann. Entomol. Soc. Am. *70*, 309–310.

Espinosa, J.S., and Stryker, M.P. (2012). Development and plasticity of the primary visual cortex. Neuron *75*, 230–249.

Ghaninia, M., Haight, K., Berger, S.L., Reinberg, D., Zwiebel, L.J., Ray, A., and Liebig, J. (2017). Chemosensory sensitivity reflects reproductive status in the ant *Harpegnathos saltator*. Sci. Rep. *7*, 3732.

Gospocic, J., Shields, E.J., Glastad, K.M., Lin, Y., Penick, C.A., Yan, H., Mikheyev, A.S., Linksvayer, T.A., Garcia, B.A., Berger, S.L., and et al. (2017). The neuropeptide corazonin controls social behavior and caste identity in ants. Cell *170*, this issue, 748–759.

Haight, K.L. (2012). Patterns of venom production and temporal polyethism in workers of Jerdon's jumping ant, Harpegnathos saltator. J. Insect Physiol. *58*, 1568–1574.

Hassan, B.A., and Hiesinger, P.R. (2015). Beyond molecular codes: simple rules to wire complex brains. Cell *163*, 285–291.

Henderson, D.S. (2004). Drosophila Cytogenetics Protocols (Humana Press).

Hölldobler, B., and Wilson, E.O. (1990). The Ants (Belknap Press of Harvard University Press).

Hölldobler, B., and Wilson, E. (2008). The Superorganism: The Beauty, Elegance, and Strangeness of Insect Societies (W. W. Norton & Company Inc.).

Hong, W., Mosca, T.J., and Luo, L. (2012). Teneurins instruct synaptic partner matching in an olfactory map. Nature *484*, 201–207.

Hoyer, S.C., Liebig, J., and Rössler, W. (2005). Biogenic amines in the ponerine ant Harpegnathos saltator: serotonin and dopamine immunoreactivity in the brain. Arthropod Struct. Dev. *34*, 429–440.

Hubel, D.H., and Wiesel, T.N. (1979). Brain mechanisms of vision. Sci. Am. *241*, 150–162.

Hummel, T., and Zipursky, S.L. (2004). Afferent induction of olfactory glomeruli requires N-cadherin. Neuron *42*, 77–88.

Imai, T., Yamazaki, T., Kobayakawa, R., Kobayakawa, K., Abe, T., Suzuki, M., and Sakano, H. (2009). Pre-target axon sorting establishes the neural map topography. Science *325*, 585–590.

Jefferis, G.S., Marin, E.C., Stocker, R.F., and Luo, L. (2001). Target neuron pre-specification in the olfactory map of Drosophila. Nature *414*, 204–208.

Jones, W.D., Cayirlioglu, P., Kadow, I.G., and Vosshall, L.B. (2007). Two chemosensory receptors together mediate carbon dioxide detection in Drosophila. Nature *445*, 86–90.

Kather, R., and Martin, S.J. (2015). Evolution of cuticular hydrocarbons in the hymenoptera: a meta-analysis. J. Chem. Ecol. *41*, 871–883.

Khila, A., and Abouheif, E. (2009). In situ hybridization on ant ovaries and embryos. Cold Spring Harb Protoc. *7*, pdb.prot5250.

Kistler, K.E., Vosshall, L.B., and Matthews, B.J. (2015). Genome engineering with CRISPR-Cas9 in the mosquito Aedes aegypti. Cell Rep. *11*, 51–60.

Koutroumpa, F.A., Monsempes, C., François, M.C., de Cian, A., Royer, C., Concordet, J.P., and Jacquin-Joly, E. (2016). Heritable genome editing with CRISPR/Cas9 induces anosmia in a crop pest moth. Sci. Rep. *6*, 29620.

Laissue, P.P., and Vosshall, L.B. (2008). The olfactory sensory map in Drosophila. Adv. Exp. Med. Biol. *628*, 102–114.

Larsson, M.C., Domingos, A.I., Jones, W.D., Chiappe, M.E., Amrein, H., and Vosshall, L.B. (2004). Or83b encodes a broadly expressed odorant receptor essential for Drosophila olfaction. Neuron *43*, 703–714.

Leonhardt, S.D., Menzel, F., Nehring, V., and Schmitt, T. (2016). Ecology and evolution of communication in social insects. Cell *164*, 1277–1287.

Li, Y., Zhang, J., Chen, D., Yang, P., Jiang, F., Wang, X., and Kang, L. (2016). CRISPR/Cas9 in locusts: Successful establishment of an olfactory deficiency line by targeting the mutagenesis of an odorant receptor co-receptor (Orco). Insect Biochem. Mol. Biol. *79*, 27–35.

Liebig, J., Hölldobler, B., and Peeters, C. (1998). Are ant workers capable of colony foundation? Naturwissenschaften *85*, 133–135.

Liebig, J., Peeters, C., Oldham, N.J., Markstädter, C., and Hölldobler, B. (2000). Are variations in cuticular hydrocarbons of queens and workers a reliable signal of fertility in the ant *Harpegnathos saltator*? Proc. Natl. Acad. Sci. USA *97*, 4124–4131.

MacLean, B., Tomazela, D.M., Shulman, N., Chambers, M., Finney, G.L., Frewen, B., Kern, R., Tabb, D.L., Liebler, D.C., and MacCoss, M.J. (2010). Skyline: an open source document editor for creating and analyzing targeted proteomics experiments. Bioinformatics *26*, 966–968.

McKenzie, S.K., Oxley, P.R., and Kronauer, D.J. (2014). Comparative genomics and transcriptomics in ants provide new insights into the evolution and function of odorant binding and chemosensory proteins. BMC Genomics *15*, 718.

McKenzie, S.K., Fetter-Pruneda, I., Ruta, V., and Kronauer, D.J. (2016). Transcriptomics and neuroanatomy of the clonal raider ant implicate an expanded clade of odorant receptors in chemical communication. Proc. Natl. Acad. Sci. USA *113*, 14091–14096.

Menuz, K., Larter, N.K., Park, J., and Carlson, J.R. (2014). An RNA-seq screen of the Drosophila antenna identifies a transporter necessary for ammonia detection. PLoS Genet. *10*, e1004810.

Mombaerts, P. (2006). Axonal wiring in the mouse olfactory system. Annu. Rev. Cell Dev. Biol. *22*, 713–737.

Nakagawa, T., Pellegrino, M., Sato, K., Vosshall, L.B., and Touhara, K. (2012). Amino acid residues contributing to function of the heteromeric insect olfactory receptor complex. PLoS ONE 7, e32372.

Nakanishi, A., Nishino, H., Watanabe, H., Yokohari, F., and Nishikawa, M. (2009). Sex-specific antennal sensory system in the ant Camponotus japonicus: structure and distribution of sensilla on the flagellum. Cell Tissue Res. 338, 79–97.

Oland, L.A., and Tolbert, L.P. (1996). Multiple factors shape development of olfactory glomeruli: insights from an insect model system. J. Neurobiol. 30, 92–109.

Omasits, U., Ahrens, C.H., Müller, S., and Wollscheid, B. (2014). Protter: interactive protein feature visualization and integration with experimental proteomic data. Bioinformatics 30, 884–886.

Ozaki, M., Wada-Katsumata, A., Fujikawa, K., Iwasaki, M., Yokohari, F., Satoji, Y., Nisimura, T., and Yamaoka, R. (2005). Ant nestmate and non-nestmate discrimination by a chemosensory sensillum. Science 309, 311–314.

Peeters, C., Liebig, J., and Holldobler, B. (2000). Sexual reproduction by both queens and workers in the ponerine ant Harpegnathos saltator. Insectes Soc. 47, 325–332.

Penick, C.A., Prager, S.S., and Liebig, J. (2012). Juvenile hormone induces queen development in late-stage larvae of the ant *Harpegnathos saltator*. J. Insect Physiol. 58, 1643–1649.

Perry, M., Kinoshita, M., Saldi, G., Huo, L., Arikawa, K., and Desplan, C. (2016). Molecular logic behind the three-way stochastic choices that expand butterfly colour vision. Nature 535, 280–284.

Petsakou, A., Sapsis, T.P., and Blau, J. (2015). Circadian rhythms in Rho1 activity regulate neuronal plasticity and network hierarchy. Cell 162, 823–835.

Riabinina, O., Task, D., Marr, E., Lin, C.C., Alford, R., O'Brochta, D.A., and Potter, C.J. (2016). Organization of olfactory centres in the malaria mosquito Anopheles gambiae. Nat. Commun. 7, 13010.

Robinson, G.E. (1987). Regulation of honey-bee age polyethism by juvenile-hormone. Behav. Ecol. Sociobiol. 20, 329–338.

Sakano, H. (2010). Neural map formation in the mouse olfactory system. Neuron 67, 530–542.

Sasaki, T., Penick, C.A., Shaffer, Z., Haight, K.L., Pratt, S.C., and Liebig, J. (2016). A simple behavioral model predicts the emergence of complex animal hierarchies. Am. Nat. 187, 765–775.

Schindelin, J., Arganda-Carreras, I., Frise, E., Kaynig, V., Longair, M., Pietzsch, T., Preibisch, S., Rueden, C., Saalfeld, S., Schmid, B., et al. (2012). Fiji: an open-source platform for biological-image analysis. Nat. Methods 9, 676–682.

Sharma, K.R., Enzmann, B.L., Schmidt, Y., Moore, D., Jones, G.R., Parker, J., Berger, S.L., Reinberg, D., Zwiebel, L.J., Breit, B., et al. (2015). Cuticular hydrocarbon pheromones for social behavior and their coding in the ant antenna. Cell Rep. 12, 1261–1271.

Sperry, R.W. (1963). Chemoaffinity in the orderly growth of nerve fiber patterns and connections. Proc. Natl. Acad. Sci. USA 50, 703–710.

Suh, H., Deng, W., and Gage, F.H. (2009). Signaling in adult neurogenesis. Annu. Rev. Cell Dev. Biol. 25, 253–275.

Sweeney, L.B., Couto, A., Chou, Y.H., Berdnik, D., Dickson, B.J., Luo, L., and Komiyama, T. (2007). Temporal target restriction of olfactory receptor neurons by Semaphorin-1a/PlexinA-mediated axon-axon interactions. Neuron 53, 185–200.

Trible, W., Chang, N., Matthews, B.J., McKenzie, S.K., Olivos-Cisneros, L., Oxley, P.R., Saragosti, J., and Kronauer, D.J. (2017). orco mutagenesis causes loss of antennal lobe glomeruli and impaired social behavior in ants. Cell 170, this issue, 727–735.

Van Oystaeyen, A., Oliveira, R.C., Holman, L., van Zweden, J.S., Romero, C., Oi, C.A., d'Ettorre, P., Khalesi, M., Billen, J., Wäckers, F., et al. (2014). Conserved class of queen pheromones stops social insect workers from reproducing. Science 343, 287–290.

Vosshall, L.B., and Hansson, B.S. (2011). A unified nomenclature system for the insect olfactory coreceptor. Chem. Senses 36, 497–498.

Vosshall, L.B., Wong, A.M., and Axel, R. (2000). An olfactory sensory map in the fly brain. Cell 102, 147–159.

Watanabe, T., Noji, S., and Mito, T. (2014). Gene knockout by targeted mutagenesis in a hemimetabolous insect, the two-spotted cricket Gryllus bimaculatus, using TALENs. Methods 69, 17–21.

Wicher, D. (2015). Olfactory signaling in insects. Prog. Mol. Biol. Transl. Sci. 130, 37–54.

Wilt, F.H., and Wessells, N.K. (1967). Methods in Developmental Biology (T.Y. Crowell Co.).

Yan, H., Simola, D.F., Bonasio, R., Liebig, J., Berger, S.L., and Reinberg, D. (2014). Eusocial insects as emerging models for behavioural epigenetics. Nat. Rev. Genet. 15, 677–688.

Yang, B., Fujii, T., Ishikawa, Y., and Matsuo, T. (2016). Targeted mutagenesis of an odorant receptor co-receptor using TALEN in Ostrinia furnacalis. Insect Biochem. Mol. Biol. 70, 53–59.

Yu, C.R., Power, J., Barnea, G., O'Donnell, S., Brown, H.E., Osborne, J., Axel, R., and Gogos, J.A. (2004). Spontaneous neural activity is required for the establishment and maintenance of the olfactory sensory map. Neuron 42, 553–566.

Zhao, N., Guan, J., Ferrer, J.L., Engle, N., Chern, M., Ronald, P., Tschaplinski, T.J., and Chen, F. (2010). Biosynthesis and emission of insect-induced methyl salicylate and methyl benzoate from rice. Plant Physiol. Biochem. 48, 279–287.

Zhou, X., Slone, J.D., Rokas, A., Berger, S.L., Liebig, J., Ray, A., Reinberg, D., and Zwiebel, L.J. (2012). Phylogenetic and transcriptomic analysis of chemosensory receptors in a pair of divergent ant species reveals sex-specific signatures of odor coding. PLoS Genet. 8, e1002930.

Zhou, X., Rokas, A., Berger, S.L., Liebig, J., Ray, A., and Zwiebel, L.J. (2015). Chemoreceptor evolution in hymenoptera and its implications for the evolution of eusociality. Genome Biol. Evol. 7, 2407–2416.

Zube, C., and Rössler, W. (2008). Caste- and sex-specific adaptations within the olfactory pathway in the brain of the ant Camponotus floridanus. Arthropod Struct. Dev. 37, 469–479.

STAR★METHODS

KEY RESOURCES TABLE

REAGENT or RESOURCE	SOURCE	IDENTIFIER
Antibodies		
Rabbit Anti-Vasa antibody	R. Lehmann's lab	N/A
Donkey anti-rabbit IgG secondary antibody, Alexa Fluor 488	ThermoFisher	Cat # A21206; RRID: AB_2535792
Chemicals, Peptides, and Recombinant Proteins		
6-methyl-5-hepten-2-one	SAFC	CAS # 110-93-0
methyl salicylate	Sigma-Aldrich	CAS # 119-36-8
1-hexanol	Sigma-Aldrich	CAS # 111-27-3 Index # 603-059-00-6
1-octen-3-ol	Sigma-Aldrich	CAS # 3391-86-4
geranyl acetate	SAFC	CAS # 105-87-3
2-heptanone	Sigma-Aldrich	CAS # 110-43-0; Index # 606-024-00-3
trans-2-hexen-1-al	Sigma-Aldrich	CAS # 6728-26-3
Paraffin oil	Sigma-Aldrich	CAS # 8012-95-1
Cas9 protein	PNA Bio Inc.	Cat # CP02
DAPI	ThermoFisher	Cat # D1306
Alexa Fluor 488 Phalloidin	ThermoFisher	Cat # A12379
Antibiotic-Antimycotic (100X)	ThermoFisher	Ref # 15240-062
BD Bacto Agar	Fisher Scientific	Ref # BD214030
Mango Taq DNA polymerase	Bioline	Cat # BIO-21083
16% paraformaldehyde solution	Electron Microscope Sciences	Cat # 15710
Critical Commercial Assays		
AmpliScribe T7-Flash Transcription kit	Epicenter	Cat # ASF3507
QIAamp DNA micro Kit	QIAGEN	Cat # 56304
pGEM-T Easy vector systems	Promega	Cat # A1360
Experimental Models: Organisms/Strains		
Harpegnathos saltator orco −/− female ants	This paper	N/A
Harpegnathos saltator orco - male ants	This paper	N/A
Harpegnathos saltator orco +/− female ants	This paper	N/A
Harpegnathos saltator wild type ants	This paper, initially from J. Liebig's lab	N/A
Oligonucleotides		
sgRNA1 (T7 promoter + target + scaffold): GTAA AACGACGGCCAGTGAATTGTAATACGACTCAC TATAGGAACTTCATGACCCTTATATGTTTAAGAG CTATGCTGGAAACAGCATAGCAAGTTTAAATAA GGCTAGTCCGTTATCAACTTGAAAAAGTGGCAC CGAGTCGGTGCTTTTTTTGTCATAGCTGTTTCCTG	Integrated DNA Technologies	gBlocks
sgRNA2 (T7 promoter + target + scaffold): GTAAA ACGACGGCCAGTGAATTGTAATACGACTCACTA TAGGAATATTTTATGCAAATACTGTTTAAGAGCT ATGCTGGAAACAGCATAGCAAGTTTAAATAAGG CTAGTCCGTTATCAACTTGAAAAAGTGGCACCG AGTCGGTGCTTTTTTTGTCATAGCTGTTTCCTG	Integrated DNA Technologies	gBlocks
PCR forward primer: tcccgtatcggcgataacgatgacaagc	Integrated DNA Technologies	Custom DNA Oligos
PCR reverse primer: tgaccgatagactaagacaggccg	Integrated DNA Technologies	Custom DNA Oligos

(Continued on next page)

Continued

REAGENT or RESOURCE	SOURCE	IDENTIFIER
Software and Algorithms		
Skyline software for Mass spectrometry	MacLean et al., 2010	N/A
Fiji	Schindelin et al., 2012	N/A
GraphPad Prism 7	GraphPad Software, La Jolla California USA	N/A
BGI *Harpegnathos saltator* genome database	Bonasio et al., 2010	Hsal_00588
NCBI database	National Center for Biotechnology Information	Gene ID: 105183395
Protter	Omasits et al., 2014	N/A
Other		
Plastic boxes (9.5 X 9.5 cm^2)	Pioneer Plastics, Inc.	Item # 028C
Plastic boxes (19 X 13.5 cm^2)	Pioneer Plastics, Inc.	Item # 079C
Plastic boxes (27 X 19 cm^2)	Pioneer Plastics, Inc.	Item # 195C
Quartz glass capillary	Sutter Instrument	Item # Q100-50-7.5
Laser-based micropipette puller	Sutter Instrument	Model # P-2000
FemtoJet ll microinjector	Eppendorf	Model # 920010504
Video recording webcam	Logitech	Model # C920
Stimulus air controller	Syntech	Model # CS-55

CONTACT FOR REAGENT AND RESOURCE SHARING

Further information and requests for reagents may be directed to and will be fulfilled by the Lead Contact, Claude Desplan (cd38@nyu.edu). Of note, the USDA permit is required for the importation and interstate movement of the wild-type and mutant ants.

EXPERIMENTAL MODEL AND SUBJECT DETAILS

Regular maintenance of *Harpegnathos* ant colonies
Harpegnathos saltator colonies were initially transported from Jürgen Liebig's laboratory at Arizona State University. Ants were maintained in plastic boxes (Pioneer Plastics, Inc.) inside the USDA approved ant room at 22-25°C. Small boxes (9.5 X 9.5 cm^2) were used to rear individually isolated workers. Medium (19 X 13.5 cm^2) and large boxes (27 X 19 cm^2) were used to rear social colonies. The floor of the boxes was made of plaster, and a glass was used in each medium or large box to separate the inside of the nest where the reproductive females and young workers (nurses) lived with the brood from outside of the nest that was the foraging area for old workers (foragers). Colonies were fed with live or pre-stung crickets 3-6 times a week. Crickets were pre-stung and subsequently paralyzed by workers in the large colonies to provide to the individually isolated ants.

Maintenance of the mutant allele and development of homozygous mutant ants
In most eusocial insects, mating cannot be achieved in the laboratory (Yan et al., 2014), but it can be carried out in *Harpegnathos* (Liebig et al., 1998). Indeed, we have successfully recorded the mating of a single male with a single virgin female of *Harpegnathos* in the lab (Movie S5). This controlled mating allowed us to generate homozygous mutants in the F4 generation (Table S1).

The mutant F1 males were identified by genotyping. Each mutant male was paired with a WT virgin female for mating under the video camera. When the mating was confirmed, the male was transferred to another nest with a new WT female to maximize the number of progeny. The male could inseminate multiple females from day 0 to day 7 after emergence. No mating was observed after day 7. The inseminated WT females gave rise to F2 heterozygotes, which in turn generated F3 hemizygous males. The mutant F3 males were backcrossed to F2s to generate F4 homozygotes (Figure 1C). Of note, as the F4s were either heterozygotes or homozygotes, the assays were performed blind without knowing their genotypes until they were harvested for genotyping.

METHOD DETAILS

Embryo injections and post-injection maintenance
Quartz glass needles were made using the P2000 Micropipette Puller (Shutter Instrument). Embryos were lined on the double-sided tape and microinjected with Cas9 proteins (0.2 μg/μl) and *in vitro* synthesized small guide RNAs (sgRNAs, 0.2 μg/μl) using the

Eppendorf FemtoJet II microinjector. The design of the sgRNAs was described previously (Perry et al., 2016), and sgRNA sequences are listed in the Key Resources Table. The *orco* (*odorant receptor co-receptor*) gene sequence (Hsal_00588 or Gene ID: 105183395) was obtained from the BGI or NCBI DNA database and the genome sequence of *Harpegnathos saltator* was reported (Bonasio et al., 2010). The structure of transmembrane domains in the Orco protein was analyzed by Protter (Omasits et al., 2014).

We first found that most injected embryos were destroyed by workers after they were re-introduced to the colony. To increase the survival rate, we optimized the method in rearing the injected embryos on 1% agar plates with 2% Antibiotic-Antimycotic (ThermoFisher Scientific) after 70% ethanol treatment (Figure S1B). After one month, when the first embryo hatched, they were transported to a nest with a few helper workers, as worker nursing is essential for the survival of larvae. The remaining embryos hatched in the colony. We fed them with pre-stung crickets to maintain stability in the small nest with injected embryos (Figures S1B and S1C).

Genotyping of embryo, larval and adult tissues

Different methods were used to analyze the genotypes of different stages of ants. First, to test somatic mutation, embryos were harvested 3 days after injections and 5 embryos were pooled for genomic DNA extraction and PCR amplification using the Taq DNA polymerase. PCR products were cloned to pGEM vector with A-T overhang (Promega). Several clones were sequenced. Second, amplified libraries were generated from extracted genomic DNA followed by MiSeq at the NYU Genomic Center to analyze the efficiency. Third, to test the germline transformation, single F1 larvae were harvested for DNA sequencing. Fourth, to test the genotype in adult males, their forewings were clipped for genomic DNA extraction and sequencing, while the individuals were alive and capable of mating with females. Fifth, to test the genotype in adult females, each individual was harvested and part of its thorax tissue was genotyped. PCR primers are indicated in the Key Resources Table.

Mass spectrometry

Proteins were extracted from antennae cleaved from WT and homozygous mutant ants. The protein extract was run on SDS-PAGE gels. Gel slices were trypsin digested followed by liquid chromatography-tandem mass spectrometry (LC-MS/MS) analysis performed at the Biological Mass Spectrometry Facility at Rutgers, The State University of New Jersey. Skyline software was used for the quantification of peak area (MacLean et al., 2010).

Immunohistochemistry of embryo nuclei and adult brain, ovary and antennae

Embryos were harvested every 4 hr from 12 hr after egg deposition (AED) to 40 hr AED. After harvesting, the embryos were boiled for 45 s, quenched quickly on ice, and fixed with 4% paraformaldehyde (PFA) supplemented with DMSO and heptane (Khila and Abouheif, 2009), followed by protocols for *Drosophila* embryo cryosectioning in the lab (30 μm thick sections).

Ant brain tissues were dissected and fixed in 4% PFA and washed three times using 1X PBS with 0.3% Triton X-100. The tissues were incubated with DAPI (2 μg/ml) and Alexa Fluor 488 Phalloidin (1/80, ThermoFisher Scientific) at room temperature for 2 hr, and then mounted and scanned using Confocal Leica TCS SP5 microscope at NYU. Images of AL glomeruli were generated using Z project in Fiji (or ImageJ). Ant ovary tissues were stained with anti-Vasa antibody (1:1000 dilution, gifted by R. Lehmann's lab) at 4°C overnight, and incubated with DAPI (2 μg/ml) and Alexa Fluor 488 anti-Rabbit secondary antibody (1:200 dilution, ThermoFisher Scientific) at room temperature for 2 hr.

The female ant antennae were dissected and fixed with 4% PFA. Flagella (Ghaninia et al., 2017) were cryosectioned (50 μm thick sections). The sections were stained with DAPI and Alexa Fluor 488 Phalloidin, and imaged using 63X objective of the Confocal Leica TCS SP5 microscope at NYU.

Behavioral responses to multiple chemicals

Each F4 ant was painted with multiple color dots on its thorax and thus named by the respective color combination (e.g., GOW was 3 colors of Green, Orange and White from anterior to posterior). Each pair of WT and F4 ants was immobilized on their thoraces (Figure S3A). Their antennae were able to move without restrictions. 20 μl of a 1% odorant/paraffin solution was transferred onto a small piece of filter paper inside a glass pipette. Seven odorants (6-methyl-5-hepten-2-one, methyl salicylate, 1-hexanol, 1-octen-3-ol, geranyl acetate, 2-heptanone, and trans-2-hexen-1-al) were delivered as a pulse into a constant 1.7l/min flow of air supplied by the building pressure gas system. The one-second pulses with a 280ml/min flow rate were controlled using a Syntech Stimulus Controller, model CS-55. The air flew directly into a Y-shaped glass tube with an inner diameter of approximately 15mm. An F4 was placed in one arm of the Y-tube and a WT into the other. The control stimuli (solvent alone) were delivered before the chemical stimuli. The antennal responses to odorant and control stimuli were video-recorded and each ant was tested for 3 rounds of the complete odorant panel. The sequence of odorants was randomized for each test, as was the position of the WT and F4 ants in the Y-tube. The videos were analyzed blind (without knowledge of the ant genotypes) and scored as follows: 0 for no retraction (or random antennae movement), 1 for mild retraction (slow or incomplete retraction), and 2 for strong retraction (quick and complete retraction). Each differential score was calculated using the score of F4 ant minus the score of paired WT ant. The Mann-Whitney test was performed for statistical analyses using GraphPad Prism 7. To predict the genotype, their responses to seven odorants were added up: 7 homozygous versus 7 heterozygous ants (1:1 ratio) were predicted based on their differential scores. This led us to make nearly 100% correct predictions of their genotypes: the only error occurred on ORRR, which appeared to be an outlier, being a heterozygote with reduced response.

Analyses of ant behavior, egg laying and lifespan

The nests for *Harpegnathos* were either separated into two areas, inside the colony (under glass) and outside the colony (Movie S3), or were relatively small and not separated (Movies S2, S4, and S5). F4 ants were grouped with WT ants that included gamergates, young workers (age < 50 days) and old workers (age > 100 days). Gamergates constantly stayed inside with young workers and brood, while normally old workers foraged, *i.e.* brought pre-stung crickets from outside to inside. The nests with two separated areas were video-recorded (Movie S3) and the time for each worker in staying outside of the colony was counted. Two-way ANOVA with Tukey's multiple comparisons test were performed for statistical analysis. For foraging, several pre-stung crickets were placed outside the colony once per day during the 17 test days (Figure 4B). Individual workers normally bring crickets from outside to inside. The foraging score was measured as the average number of pre-stung crickets brought to the nest by WT old, WT young, heterozygous young, and homozygous young worker ants (total number of crickets divided by the number of individuals in each genotype/age category). Friedman test with Dunn's multiple comparisons test were performed for statistical analysis.

To observe behaviors, reproduction and lifespan for solitary female ants, individual F4s were isolated to generate gamergates. Their behaviors were video-recorded and their brood was counted weekly. The videos were analyzed manually and blind. Mann-Whitney and Fisher's exact tests were performed for statistical analyses of abnormal antennal movement, individual egg-laying and larvae-containing colonies. For the lifespan analysis in males, 32 WT and 31 hemizygous mutant ants in the F3 generation were compared, and the unpaired t test was performed for statistical analysis.

To address the role of Orco in the dueling and gamergate transition, we generated a colony (n = 39) with homozygous and heterozygous young workers, without gamergates. The frequency of dueling was observed 6 times per day (each time for 30 min) during the first 9 days after dueling started. The gamergates were determined by their egg-laying 3 months after separation. The statistical analysis of dueling and gamergate transition in the heterozygous versus homozygous ants was performed using Fisher's exact test, and the dueling frequencies in the heterozygous versus homozygous duelers were performed using Wilcoxon matched-pairs signed rank test.

Measurement of antennal lobes

Confocal microscopy was used to visualize whole mount brains dissected from old female *Harpegnathos* ants (∼3 months old) using DAPI and Alexa Fluor® 488 Phalloidin. Glomeruli were reconstructed from image stacks using the segmentation editor of the Fiji (Schindelin et al., 2012). The AL areas were manually determined by the outlines of the clusters of glomeruli. The glomerular volume of each AL was analyzed by the Object Counter 3D Fiji plugin (Bolte and Cordelières, 2006), and normalized by the volume of central region (protocerebrum) of the same brain, including protocerebral neutrophil, vertical lobe, peduncle and central bodies (Hoyer et al., 2005). The volumes of the left and right ALs were averaged to find each individual's AL volume. For the counting of glomeruli number, each glomerulus was identified in the image stack and tracked with a manually placed high intensity mark using Fiji. The glomeruli counts in the left and right ALs were averaged to obtain the count per lobe in each organism. To measure the size of glomeruli, an AL per individual ant was reconstructed from image stacks using Fiji. Multiple glomeruli in each AL were picked at random (27 glomeruli per female ant, and 3-14 per male ant depending on the location of glomeruli: 3 for dorsal glomeruli, 5 for medium size ventral glomeruli, and 14 for small size ventral glomeruli). The 3D image was calibrated with zoom settings and a line was drawn across the shortest midsections. The length of each line was measured using Fiji, and was averaged for each AL. Similar methods were used to quantify the glomerular volume and number of glomeruli in eight ALs in male ants, as well as the measurements in newly eclosed female ants. One-way ANOVA with Tukey's multiple comparisons test were performed for old female ants and unpaired t test for male and newly eclosed female ants in the statistical analyses using GraphPad Prism 7.

QUANTIFICATION AND STATISTICAL ANALYSIS

Statistical analyses including unpaired t test, Mann-Whitney test, one-way or two-way ANOVA with Tukey's multiple comparisons test, Fisher's exact test, Wilcoxon matched-pairs signed rank test, and Friedman test with Dunn's multiple comparisons test are indicated in Method Details and Figure Legends. The value of n, mean ± SEM, and p value are reported in Results, Figures, and Figure Legends. Statistically significance is defined by $p < 0.05$. Statistical analysis was performed using GraphPad Prism 7.

Supplemental Figures

Cell
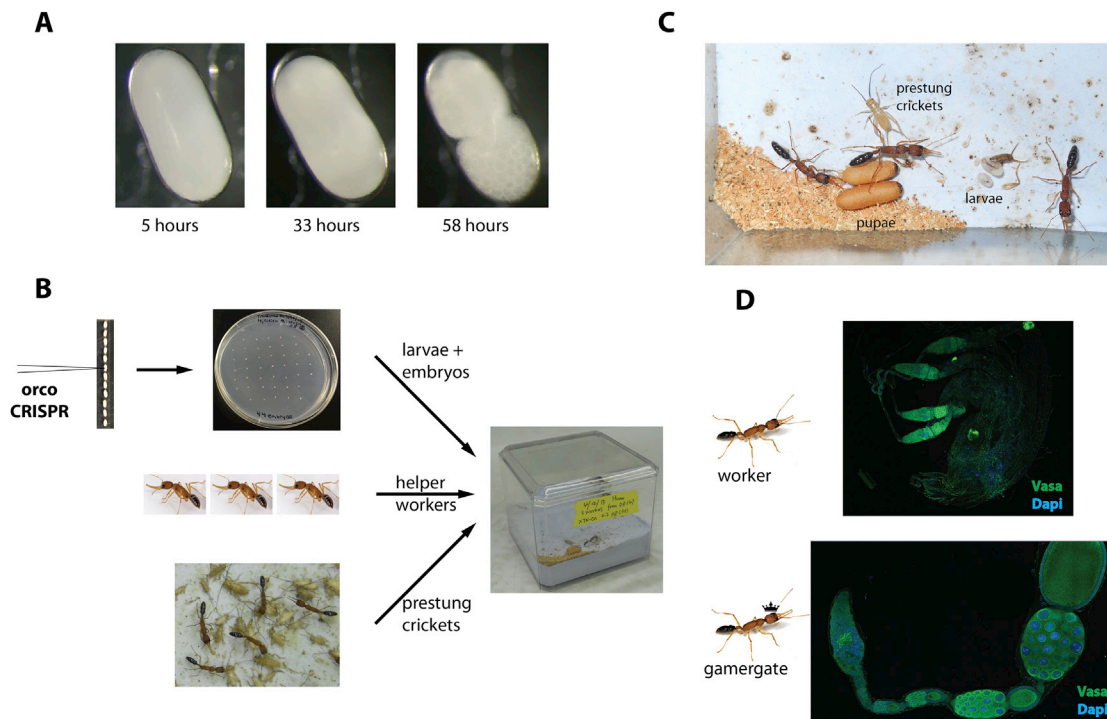
Figure S1. Embryo Development, Injections, and Maintenance and the Worker-to-Gamergate Transition in *Harpegnathos saltator*, Related to Figure 1

(A) A *Harpegnathos* young embryo was placed in mineral oil. Photos were taken under a dissection microscope at different time points after egg deposition (AED). The contraction of the vitelline membrane from the chorion at 33 hr AED indicated that the embryo was still at the syncytial stage (Wilt and Wessells, 1967). The embryo at 58 hr AED reached gastrulation.

(B) After injections, embryos were removed from the double-sided tape and placed on an agar plate. After one month, they were transported to a colony with 3 nursing workers. The colony was fed with pre-stung crickets.

(C) Later on, the larvae and pupae developed from the injected embryos.

(D) The ovaries dissected from worker versus gamergate indicated that egg chambers and oocytes grow in the gamergate, while the ovary growth is arrested in the worker. Vasa: green; DAPI: blue.

A

AGAATATTTTATGCAAATACTTGGACGAATTATCATCGTAATAATTGAATACAAAGTGGCCGAAGAACTTCATGACCCTTATATTGGGCAA

```
AGAATATTTTATGCAAA-------------------------------------------------------------TATTGGGCAA
AGAATATTTTATGCAA--------------------------------------------------------------TATTGGGCAA
AGAATATTTTATGCAA---------------------------------------------------------------ATTGGGCAA
AGAATATTTTATGCAA---------------------------------------------------------------T-TTGGGCAA
```

B

C

D

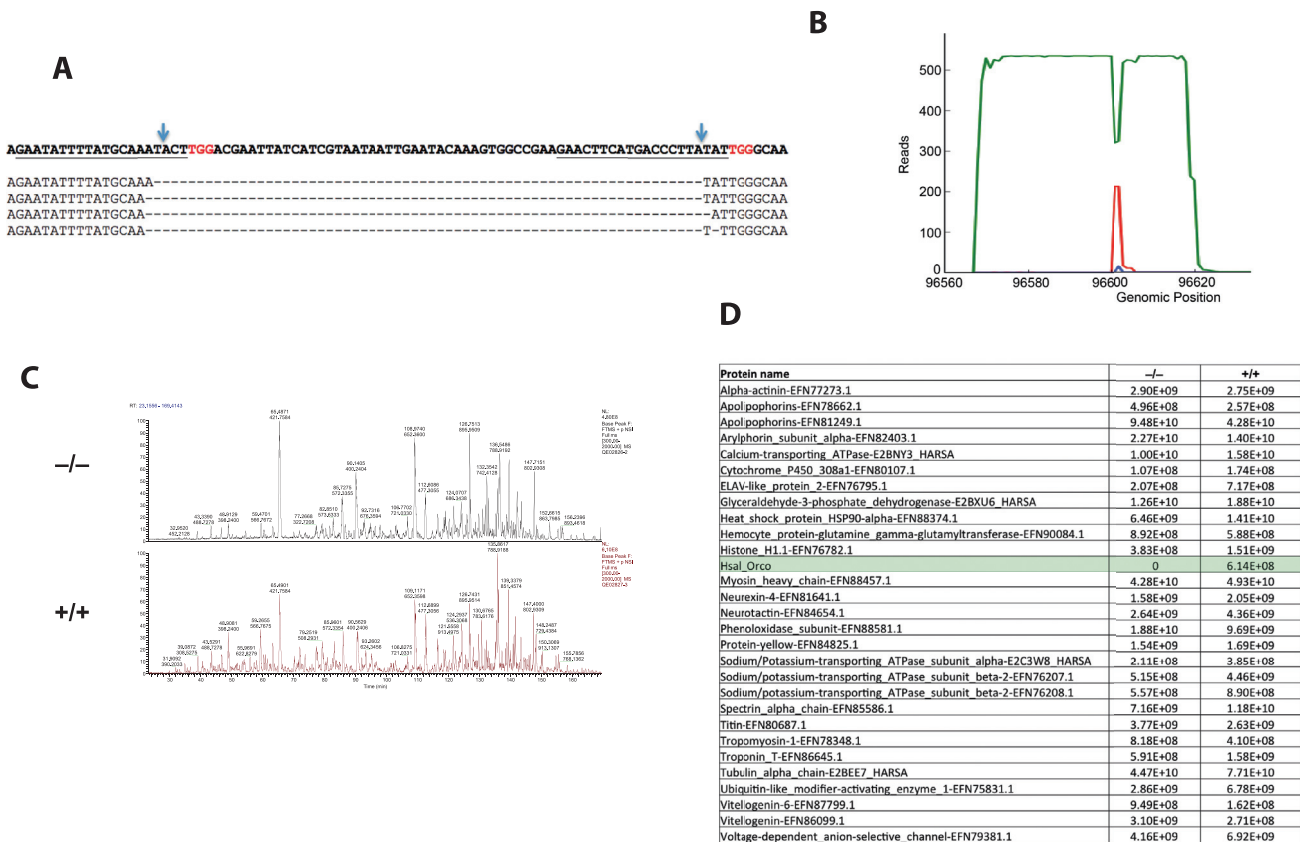| Protein name	–/–	+/+
Alpha-actinin-EFN77273.1	2.90E+09	2.75E+09
Apolipophorins-EFN78662.1	4.96E+08	2.57E+08
Apolipophorins-EFN81249.1	9.48E+10	4.28E+10
Arylphorin_subunit_alpha-EFN82403.1	2.27E+10	1.40E+10
Calcium-transporting_ATPase-E2BNY3_HARSA	1.00E+10	1.58E+10
Cytochrome_P450_308a1-EFN80107.1	1.07E+08	1.74E+08
ELAV-like_protein_2-EFN76795.1	2.07E+08	7.17E+08
Glyceraldehyde-3-phosphate_dehydrogenase-E2BXU6_HARSA	1.26E+10	1.88E+10
Heat_shock_protein_HSP90-alpha-EFN88374.1	6.46E+09	1.41E+10
Hemocyte_protein-glutamine_gamma-glutamyltransferase-EFN90084.1	8.92E+08	5.88E+08
Histone_H1.1-EFN76782.1	3.83E+08	1.51E+09
Hsal_Orco	0	6.14E+08
Myosin_heavy_chain-EFN88457.1	4.28E+10	4.93E+10
Neurexin-4-EFN81641.1	1.58E+09	2.05E+09
Neurotactin-EFN84654.1	2.64E+08	4.36E+08
Pheroloxidase_subunit-EFN88581.1	1.88E+10	9.69E+09
Protein-yellow-EFN84825.1	1.54E+09	1.69E+09
Sodium/Potassium-transporting_ATPase_subunit_alpha-E2C3W8_HARSA	2.11E+08	3.85E+08
Sodium/potassium-transporting_ATPase_subunit_beta-2-EFN76207.1	5.15E+08	4.46E+09
Sodium/potassium-transporting_ATPase_subunit_beta-2-EFN76208.1	5.57E+08	8.90E+08
Spectrin_alpha_chain-EFN85586.1	7.16E+09	1.18E+10
Titin-EFN80687.1	3.77E+09	2.63E+09
Tropomyosin-1-EFN78348.1	8.18E+08	4.10E+08
Troponin_T-EFN86645.1	5.91E+08	1.58E+09
Tubulin_alpha_chain-E2BEE7_HARSA	4.47E+10	7.71E+10
Ubiquitin-like_modifier-activating_enzyme_1-EFN75831.1	2.86E+09	6.78E+09
Vitelogenin-6-EFN87799.1	9.49E+08	1.62E+08
Vitelogenin-EFN86099.1	3.10E+09	2.71E+08
Voltage-dependent_anion-selective_channel-EFN79381.1	4.16E+09	6.92E+09

Figure S2. Somatic and Germline Mutations in *orco*, Related to Figure 2

(A) Somatic mutagenesis with two sgRNAs (sgRNA1 and sgRNA2) generated deletions of ∼60 nucleotides in length.

(B) MiSeq sequencing shows that the somatic mutation rate of sgRNA1 is approximately 40%. The green line indicates wild-type (WT) sequence, while the red and blue lines indicate deletions and point mutations, respectively. Surrounding the target site (genomic position 96003), the WT reads start to decrease, and the mutations start to increase, with the majority of mutations being short deletions.

(C and D) Mass spectrometry indicates that no protein could be detected in the antennae of *orco* F4 homozygous mutant. The LC-MS/MS basepeak chromatograms indicate that overall peak profiles are similar in the WT and homozygous female antennae (C). Moreover, the quantifications of peak area in multiple proteins indicate that Orco protein was abundant in the WT antennae but its expression was completely abolished in the homozygote (D).
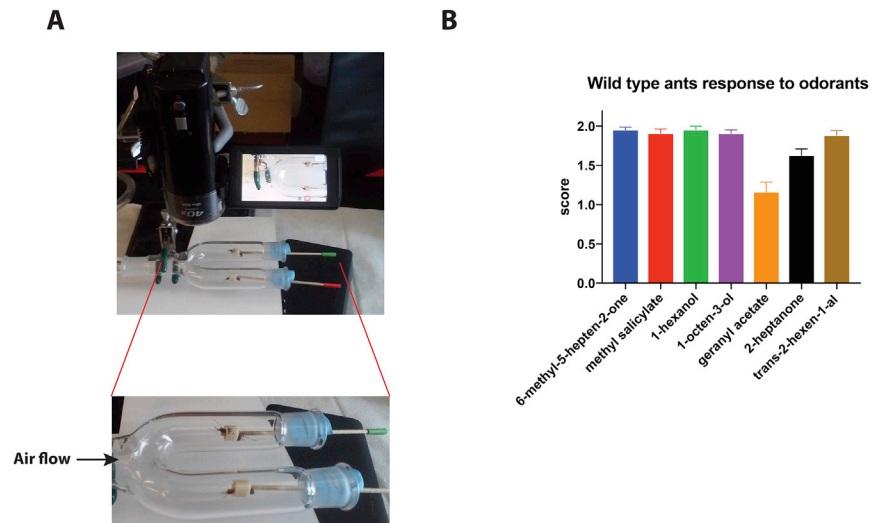
A

B

Wild type ants response to odorants

Figure S3. Antennal Retraction in Response to General Odorants, Related to Figure 3

(A) The experimental setting: two ants (one F4 and one WT) were placed in the Y-shape glass tube. Antennal responses to the puff of certain odorants were recorded and scored before knowing the genotypes of F4 ants.

(B) Average responses of the 14 wild-type ants (3 tests for each ant) to the general odorants (no response: 0; mild response: 1; strong response: 2). Data are represented as mean ± SEM.
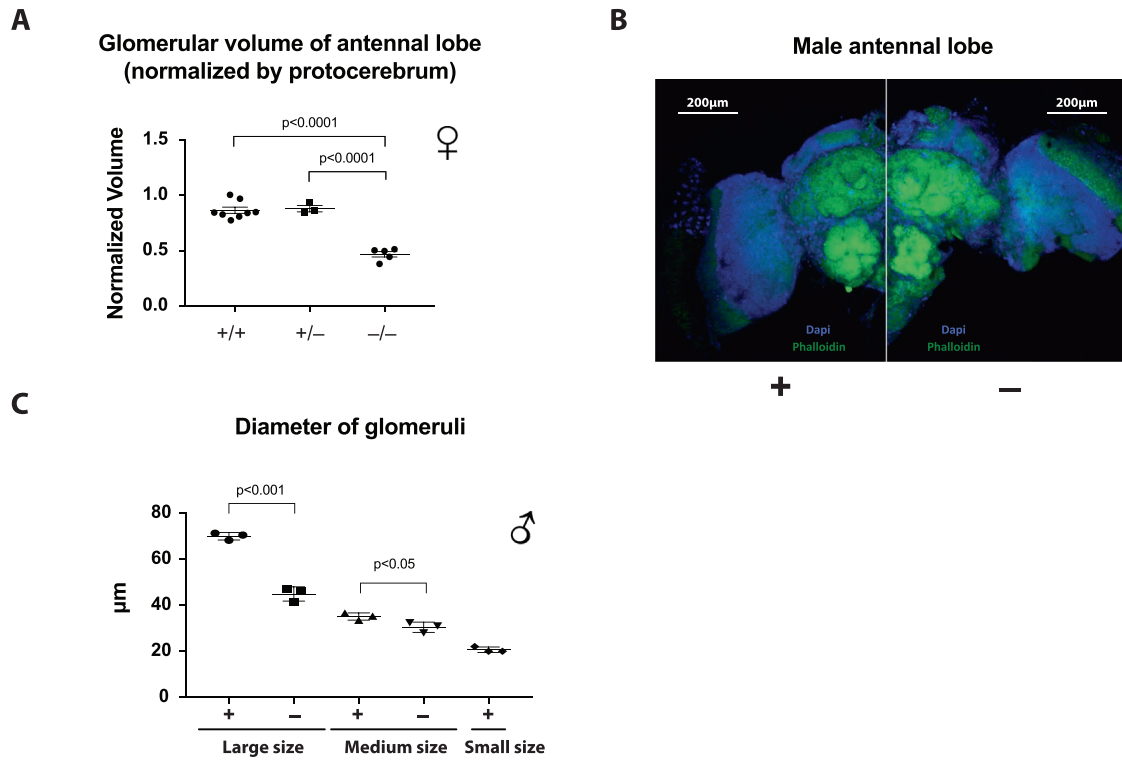
A

Glomerular volume of antennal lobe
(normalized by protocerebrum)

B

Male antennal lobe

C

Diameter of glomeruli

Figure S4. Neuroanatomical Phenotypes in Female and Male Mutant Ants, Related to Figure 6

(A) Normalized glomerular volume of antennal lobe in WT (+/+, n = 8), heterozygous (+/−, n = 3), and homozygous female ants (−/−, n = 5).

(B) The confocal images of wild-type (+) versus mutant males (-): Phalloidin (green), DAPI (blue), 10X objective.

(C) The diameter of dorsal glomeruli in WT (n = 3): 69.80 ± 0.93 μm and mutant males (n = 3): 44.73 ± 1.78 μm. The ventral glomeruli in WT are separated into two groups: medium size glomeruli: 34.93 ± 0.90 μm and small size glomeruli: 20.50 ± 0.70 μm. The medium size glomeruli in mutant ants: 30.27 ± 1.30 μm, while small glomeruli were not observed in mutant ants. p values are indicated for each plot. Data are represented as mean ± SEM.
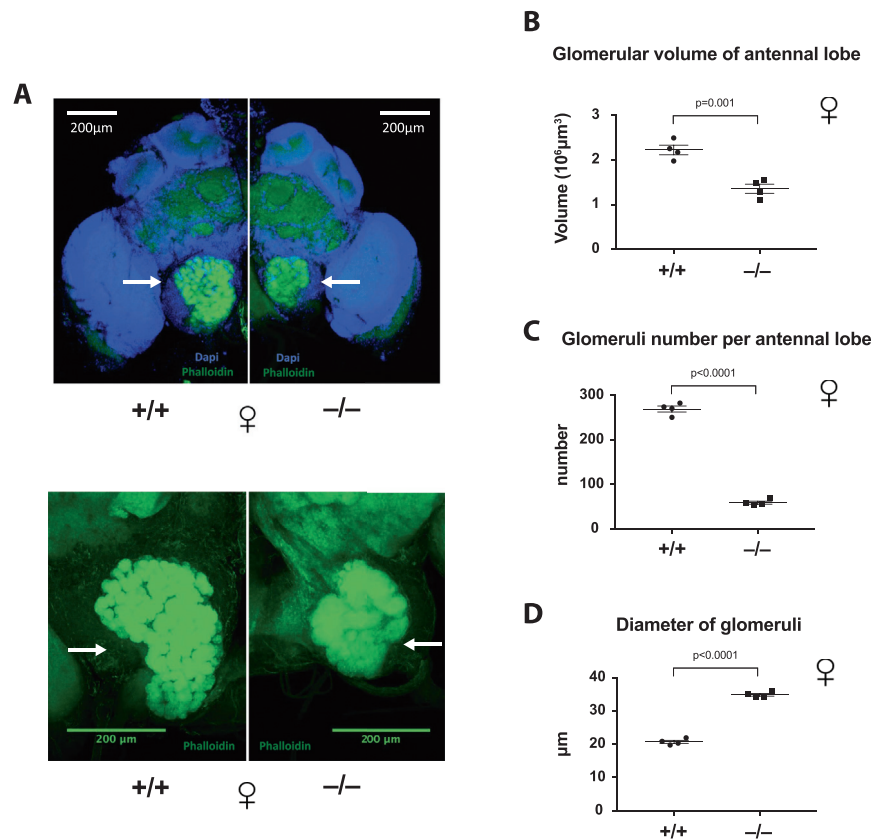
Figure S5. Neuroanatomical Phenotypes in Newly Enclosed Female Ants, Related to Figure 6

(A) Confocal images of WT (+/+) versus homozygous mutant brains (−/−) in young female ants (< 1 day old): 10X objective (top panel) and 20X objective (bottom panel). The glomerular areas of antennal lobes are indicated by arrows. Phalloidin (green), DAPI (blue).

(B) The average glomerular volume of left and right antennal lobes in WT (n = 4): $2.23 \pm 0.11 \times 10^6\ \mu m^3$ and homozygous female ants (n = 4): $1.36 \pm 0.10 \times 10^6\ \mu m^3$.

(C) The number of glomeruli in WT: 269.4 ± 6.8 and homozygous female ants: 59.0 ± 3.4.

(D) The diameter of glomeruli in WT: $20.7 \pm 0.5\ \mu m$ and homozygous female ants: $34.8 \pm 0.4\ \mu m$. Data are represented as mean $\pm$ SEM.